

12.1	Introduction	445
12.2	Hazards of Electromagnetic Radiation to Personnel (HERP)	
12.3	Hazards of Electromagnetic Radiation to Ordnance (HERO)	
12.4	Hazards of Electromagnetic Radiation to Fuel (HERF)	
12.5	Radiation Hazard Levels for Personnel	446
12.6	Radiation Hazard Limits	448
12.7	Radiation Protection	449
	Exercises	449
	References	450

13. Microwave Measurements

13.1	Introduction	451
13.2	Tunable Detector	451
13.3	Slotted Line Carriage	453
13.4	VSWR Meter	454
13.5	Spectrum Analyser	454
13.6	Network Analyser	456
13.7	Power Measurements	459
13.8	Insertion Loss and Attenuation Measurements	464
13.9	VSWR Measurements	466
13.10	Return Loss Measurement by a Reflectometer	
13.11	Impedance Measurement	473
13.12	Frequency Measurement	478
13.13	Measurement of Cavity Q	480
13.14	Dielectric Constant Measurement of a Solid	491
13.15	Measurements of Scattering Parameters of a Network	497
13.16	Microwave Antenna Measurements	501
13.17	Radar Cross-Section (RCS) Measurements	507
	Exercises	509
	References	510

Index

Scattering Parameters ?? 513

MICROWAVE MEASUREMENTS

13.1 INTRODUCTION

The basic measurement parameters in low frequency ac circuits containing lumped elements are voltage, current, frequency and true power. From these measurements, the values of the impedance, the power factor, and the phase angle can be calculated. At microwave frequencies, the amplitudes of the voltages and currents on a transmission line are functions of distance and are not easily measurable. However, in a lossless line, the power transmitted is independent of the location along the line. Therefore, it is more convenient to measure power instead of voltage and current. Much of the properties of devices and circuits at microwave frequencies are obtained from the measurement of S-parameters, power, frequency, phase shift, VSWR and the noise figure.

Due to the complications and high cost of direct microwave measuring devices and instrumentations, such as, vector network analysers, spectrum analysers, power meters, etc., microwave measurements in the laboratory are often carried out using 1 kHz square-wave modulating signal which modulates the microwave test signal. The transmitted and reflected signals are then demodulated and measured using low frequency instruments such as an oscilloscope and a low frequency (1kHz) tuned receiver, called VSWR meter. The amplitude and phase information of the microwave test signals are available in the detected low frequency signal for calculating the desired parameters. These are described in the following sections. It is found appropriate to include the descriptions of some important measurement devices and instrumentations in brief, in this chapter.

13.2 TUNABLE DETECTOR

The low frequency square-wave modulated microwave signal is detected using non-reciprocal detector diode mounted in the microwave transmission line. These diodes are specially designed point contact or metal-semi conductor Schottky barrier diodes. A detailed description of these diodes are given in Chapter 10. To match the detector to the transmission system a tunable stub is used as shown in Fig. 13.1. Broad band detectors are also manufactured in coaxial form. In order to pick up propagating fields, a coaxial line tunable probe detector is used.

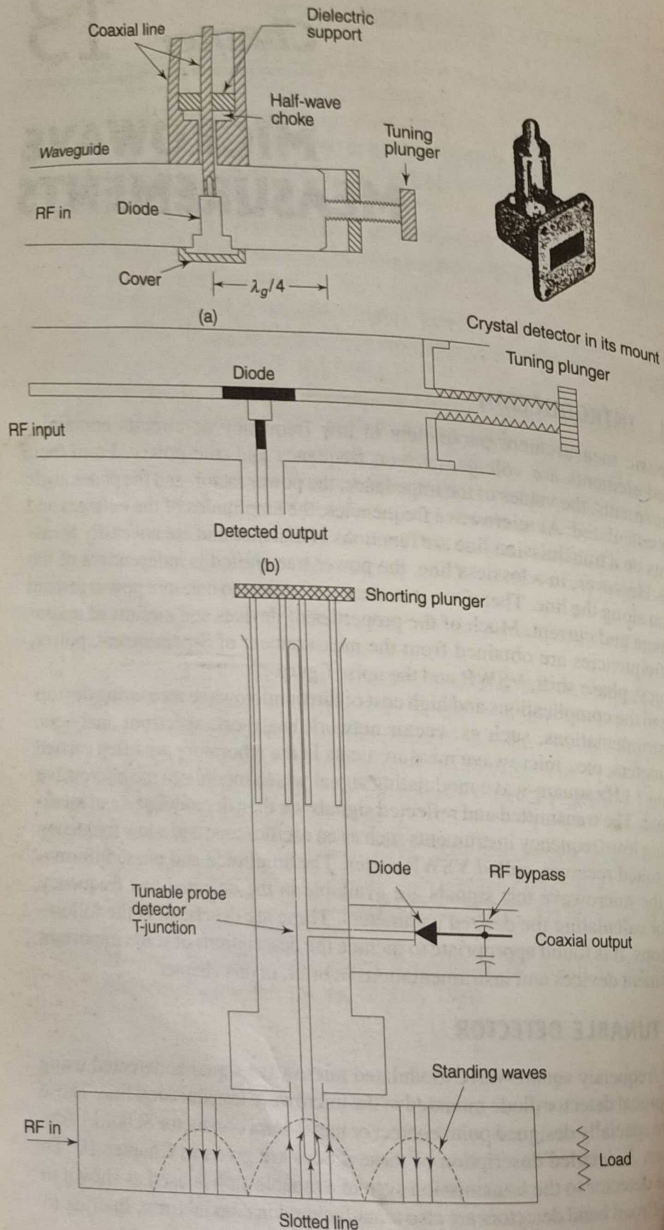
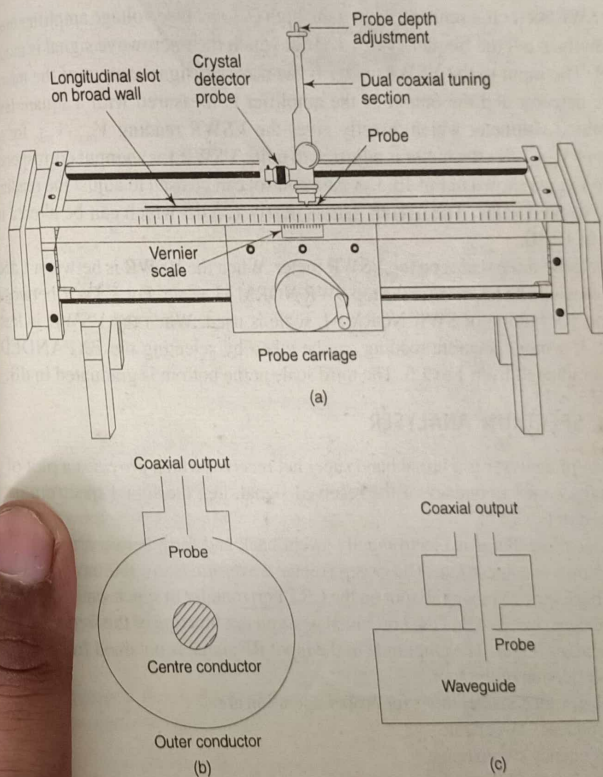


Fig. 13.1 (a) Tunable waveguide detector (b) Coaxial detector
(c) Tunable probe detector

13.3 SLOTTED LINE CARRIAGE

A slotted line carriage (Fig. 13.2) contains a coaxial E-field probe which penetrates inside a rectangular waveguide slotted section or a coaxial slotted line section from the outer wall and is able to traverse a longitudinal narrow slot. The longitudinal slot is cut along the centre of the waveguides broad wall or along the outer conductor of the coaxial line over a length of 2-3 wavelengths where the electric current on the wall does not have any transverse component. The slot should be narrow enough to avoid any distortion in the original field inside the waveguide. The two ends of the slot is tapered to zero width for reducing the effect of discontinuity. The probe is made to move longitudinally at a constant small depth to achieve a uniform coupling coefficient between the electric field inside the line and the probe current at all positions. The probe samples the elec-



13.2 (a) Slotted line carriage and schematic diagram (b) Cross-section of a coaxial slotted line (c) Cross-section of rectangular waveguide slotted line (d) Longitudinal slot and electric wall currents

tric field which is proportional to the probe voltage. This unit is primarily used for the determination of locations of voltage standing wave maxima and minima along the line. The probe carriage contains a stub tunable coaxial probe detector to obtain a low frequency modulating signal output to a scope or VSWR meter. The probe should be very thin compared to the wavelength and the depth also should be small enough to avoid any field distortion.

The slotted line with tunable probe detector is used to measure

1. VSWR and standing wave pattern
2. Wavelength
3. Impedance, reflection coefficient and return loss measurements by the minima shift method.

13.4 VSWR METER

A VSWR meter is a sensitive high gain, high Q , low noise voltage amplifier tuned normally at a fixed frequency of 1 KHz at which the microwave signal is modulated. The input to the VSWR meter is the detected signal output of the microwave detector and the output of the amplifier is measured with a square-law-calibrated voltmeter which directly gives the VSWR reading V_{\max}/V_{\min} for an input of V_{\min} , after the meter is adjusted to unity VSWR for an input corresponding to V_{\max} as shown in Fig.13.3. A gain control can be used to adjust the reading to the desired value. The overall gain is nearly 125 dB which can be altered in steps of 10 dB.

There are three scales on the VSWR meter. When the VSWR is between 1 and 4, reading can be taken from the top SWR NORMAL scale. For VSWR between 3.2 and 10, bottom of SWR NORMAL scale is used. When the VSWR is less than 1.3, a more accurate reading can be taken by selecting the EXPANDED scale, graduated from 1 to 1.3. The third scale at the bottom is graduated in dB, scale, graduated from 1 to 1.3. The third scale at the bottom is graduated in dB.

13.5 SPECTRUM ANALYSER

A spectrum analyser is a broad band super heterodyne receiver which provides a plot of amplitude versus frequency of the received signal, i.e., the signal spectrum as explained in Fig.13.4.

The local oscillator is electronically swept back and forth between two frequency limits at a linear rate. The sweep voltage waveform is saw tooth type with zero flyback time to move the spot on the CRT horizontally in synchronism with the frequency sweep so that the horizontal position is a function of the frequency of the local oscillator. The amplitude of the input RF signal is obtained from the vertical deflection of the spot.

The basic design considerations for proper operation are:

1. Frequency sweep rate
2. Frequency sweep range
3. Bandwidth of IF amplifier
4. Centre frequency of IF amplifier.

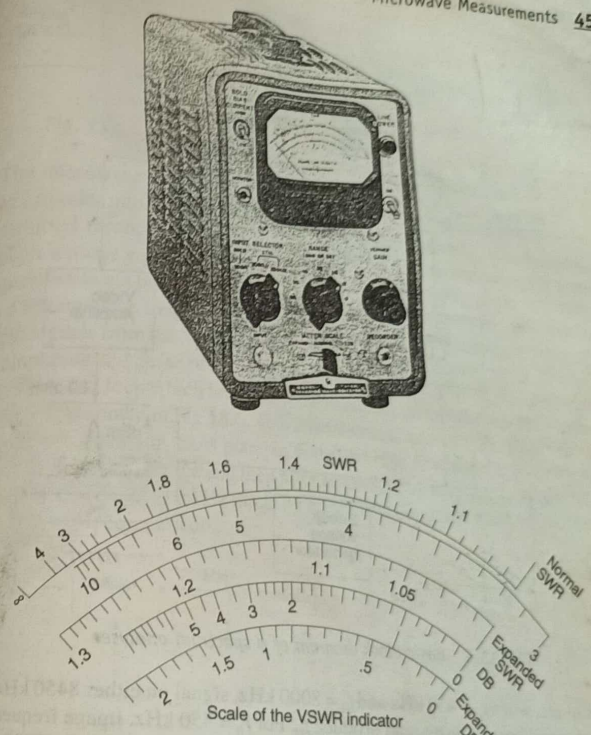


Fig. 13.3 VSWR meter (Courtesy : Hewlett Packard)

For highest resolution, the bandwidth should be kept minimum and consequently sweep speed should be very low in order to allow time to build up the voltage in the receiver circuit. The range of frequencies to be covered should be small as possible. The IF frequency should be chosen high enough to avoid the image response. If f_i is image frequency, f_0 is local oscillator frequency, f_{if} is IF frequency and f_s is signal frequency, then

$$f_i = f_0 \pm f_{if} = f_s \pm 2f_{if} \quad (13.1)$$

the frequency that beats with the L.O. frequency and produces a frequency difference equal to the IF. Thus

$$f_{if} = f_s - f_0 ; f_s > f_0 \quad (13.2)$$

$$= f_0 - f_s ; f_s < f_0 \quad (13.3)$$

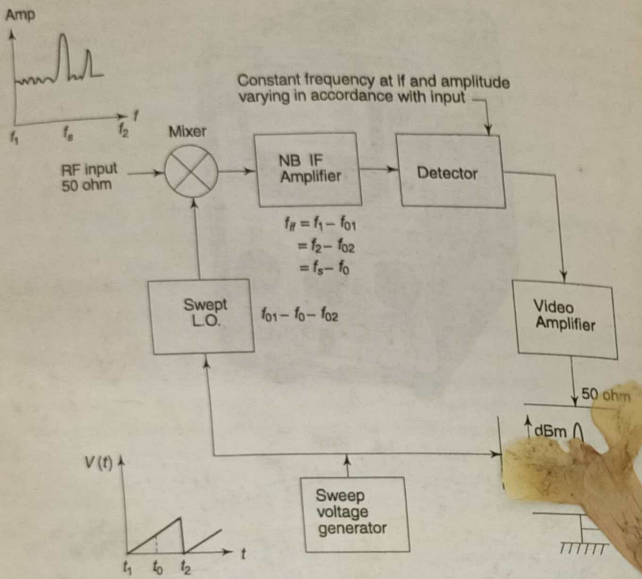


Fig. 13.4 Basic block diagram of a spectrum analyser

For example, when $f_{if} = 450$ kHz and $f_0 = 8000$ kHz, signal on either 8450 kHz or 7550 kHz will beat against f_0 and produce f_{if} . For $f_{if} = 450$ kHz, image frequency $f_i = 450 \times 2 = 900$ kHz off the signal frequency. For $f_{if} = 2000$ kHz, $f_i = 2000 \times 2 = 4$ MHz off the signal and can be tuned out easily.

The bandwidth and hence resolution of the spectrum analyser is determined by the bandwidth of IF amplifier.

13.6 NETWORK ANALYSER

The use of the slotted line for microwave measurements has the disadvantage that the amplitude and phase measurements are limited to single frequencies. Therefore, broadband testing is very time consuming and manpower cost is very high. A network analyser measures both amplitude and phase of a signal over a wide frequency range within a reasonable time. The basic measurements involve an accurate reference signal which must be generated with respect to which the test signal amplitude and phase are measured. A schematic block diagram of a complex network analyser is shown in Fig. 13.5.

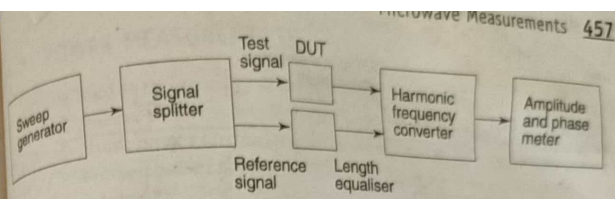


Fig. 13.5 Schematic block diagram of a complex network analyser

The microwave signal from a sweep oscillator is first divided by means of a power divider into test signal and a reference signal channel. The test signal is transmitted through the device under test, while the reference signal passes through a phase equalising length of line. Since processing of the microwave frequencies is not practical, both the test and reference signals are converted to a fixed intermediate frequency by means of a harmonic frequency converter. The output signals from the harmonic frequency converter are compared to determine the amplitude and phase of the test signal. The harmonic frequency converter uses a phase locked loop which helps the local oscillator to track the reference channel frequency as shown in Fig. 13.6. This allows swept frequency measurements. The frequency conversion takes place in two steps. The first mixer converts RF to a fixed IF in the MHz range and then after amplification they are further converted to another fixed IF in the kHz range by means of second mixer for the final amplitude and phase comparison.

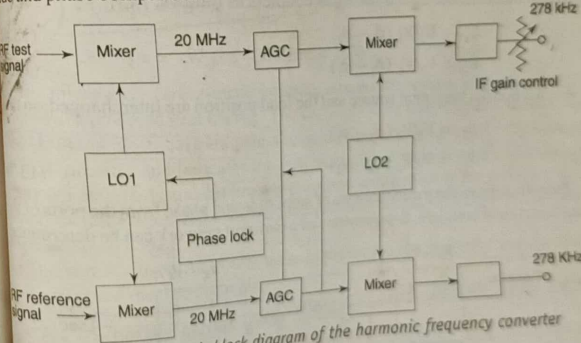


Fig. 13.6 Schematic block diagram of the harmonic frequency converter

The reflection and transmission measurements are carried out by using the reflection-transmission test unit as shown schematically in Fig. 13.7. The reference line length can be balanced for transmission measurement, and the device under test is compared to the sliding short for reflection measurements. The direction couplers used in the bridge are accurately matched to ensure a good balance between the two channels.

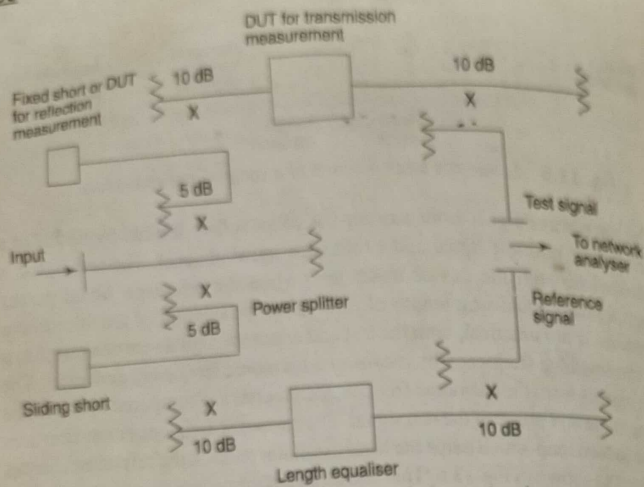


Fig. 13.7 Reflection-transmission test unit

For a two port-network, Fig. 13.8 shows the test set up for S-parameters S_{11} , and S_{21} measurements using a network analyser S_{ii} and S_{ij} are computed from the measured output of the dual directional couplers as follows:

$$S_{11} = V_2/V_1 (\phi_2 - \phi_1) \quad (13.4)$$

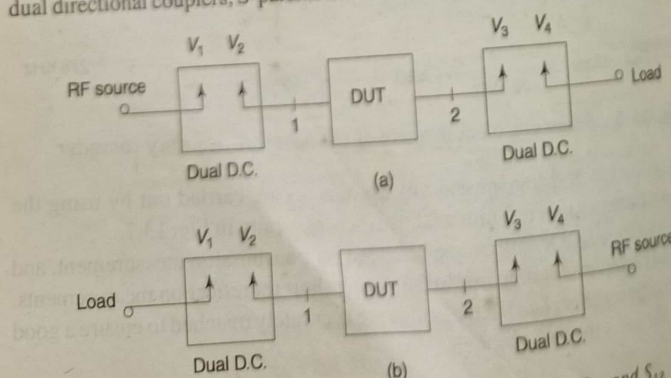
$$S_{21} = V_3/V_1 (\phi_3 - \phi_1) \quad (13.5)$$

For S_{22} and S_{12} the signal source and the load position are interchanged, so that

$$S_{22} = V_3/V_4 (\phi_3 - \phi_4) \quad (13.6)$$

$$S_{12} = V_2/V_4 (\phi_2 - \phi_4) \quad (13.7)$$

Therefore, from the measurements of amplitude and phase from the ports of the dual directional couplers, S-parameters of a two-port network can be determined.

Fig. 13.8 S-parameter test set (a) S_{11} and S_{21} (b) S_{22} and S_{12}

13.7 POWER MEASUREMENTS

Power is defined as the quantity of energy dissipated or stored per unit time. The range of microwave power is divided into three categories—low power (less than 10 mW), medium power (from 10 mW to 10 W) and high power (greater than 10 W). The average power is measured while propagation in a transmission medium and is defined by.

$$P_{av} = \frac{1}{nT} \int_0^{nT} v(t) i(t) dt \quad (13.8)$$

where T is the time period of the lowest frequency involved in the signal and n cycles are considered. For a pulsed signal

$$P_{peak} = \frac{1}{\tau} \int_0^{\tau} v(t) i(t) dt \quad (13.9)$$

$$P_{av} = P_{peak} * \text{Duty cycle} \quad (13.10)$$

$$\text{Duty cycle} = \text{pulse width} * p.r.f = \tau f_r = \tau/T < 1$$

where τ is the pulse width, T is the period and f_r is the pulse repetition frequency. The most convenient unit of power at microwaves is dBm, where

$$P(\text{dBm}) = 10 \log \frac{P(\text{mW})}{1 \text{mW}} \quad (13.11)$$

$$30 \text{ dBm} = 1 \text{W} \text{ and } -30 \text{ dBm} = 1 \mu\text{W}.$$

The microwave power meter consists of a power sensor, which converts the microwave power to heat energy. The corresponding temperature rise provides a change in the electrical parameters resulting in an output current in the low frequency circuitry and indicates the power. High power is often measured especially for standards and calibration purposes, using microwave calorimeters in which the temperature rise of the load provides a direct measure of the power absorbed by the load.

The sensors used for power measurements are the Schottky barrier diode, bolometer and the thermocouple.

13.7.1 Schottky Barrier Diode Sensor

A zero-biased Schottky barrier diode is used as a square-law detector whose output is proportional to the input power. Since diode resistance is a strong function of temperature, the circuit is designed such that the input matching is not affected by diode resistance as shown by the equivalent circuit in Fig. 13.9. The diode detectors can be used to measure power levels as low as 70 dBm.

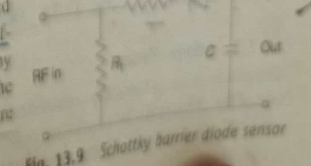


Fig. 13.9 Schottky barrier diode sensor

13.7.2 Bolometer Sensor

A bolometer is a power sensor whose resistance changes with temperature as it absorbs microwave power. The two most common types of bolometer are, the barretter and the thermistor. The barretter is a short thin metallic (Platinum) wire sensor which has a positive temperature coefficient of resistance. The thermistor is a semiconductor sensor which has a negative temperature coefficient of resistance and can be easily mounted in microwave lines as shown in Fig. 13.10 due to its smaller and more compact size. The impedances of these bolometers are in the range 100–200 ohm. However, barretters are more delicate than thermistors, hence they are used only for very low power (< few mW). Medium and high power are measured with a low-power thermistor sensor, after precisely attenuating the signal. The sensitivity level of a thermistor is limited to about 20 dBm. The thermistor mount provides good impedance match, low loss, good isolation from thermal and physical shock and good shielding against energy leakage.

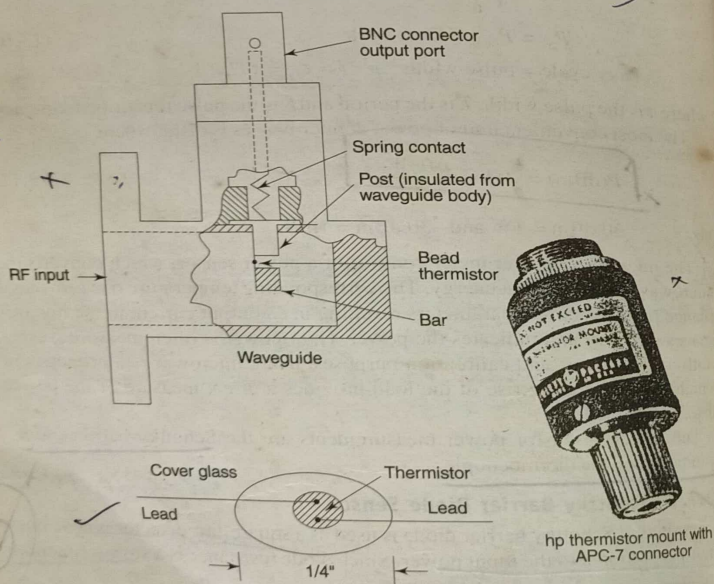
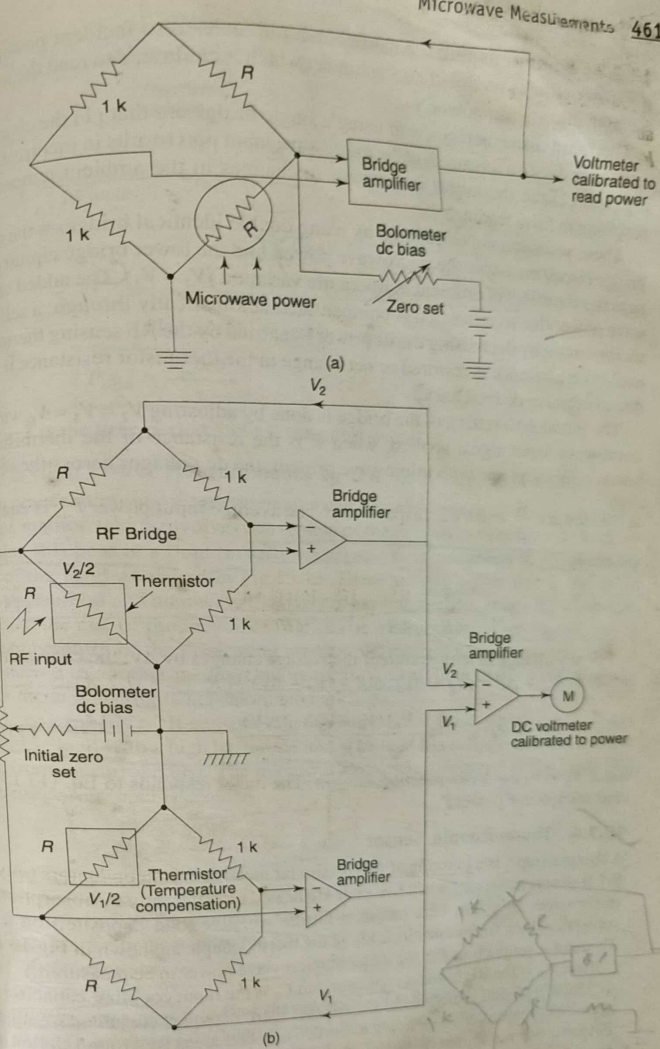


Fig. 13.10 Thermistor mount

13.7.3 Power Meter

The power meter is basically constructed from a balanced bridge circuit in which one of the arms is the bolometer as shown in Fig. 13.11. The microwave power applied to this arm will change the bolometer's resistance causing an unbalance

Fig. 13.11 Principle of the power meter bridge circuit (a) Single bridge
(b) Double bridge for compensation

In its initial balance condition under zero incident power, the output is recorded on a voltmeter which is calibrated to read the level of the input microwave power. The main disadvantages with using a single bridge are that (1) the change of resistance due to a mismatch at the microwave input port results in incorrect reading and (2) the thermistor is sensitive to changes in the ambient temperature resulting in false reading.

These problems are eliminated by using double identical bridges—the upper bridge circuit measures the microwave power, and the lower bridge circuit compensates the effect of ambient temperature variation ($V_1 = V_2$). The added microwave power due to mismatch is compensated automatically through a self-balancing circuit by decreasing the dc power V_2 carried by the RF sensing thermistor until bridge balance is restored or net change in the thermistor resistance is zero due to negative dc feed back.

The initial zero setting of the bridge is done by adjusting $V_2 = V_1 = V_0$ with no microwave input signal applied, when R is the resistance of the thermistor at balance. Without and with microwave present, the dc voltages across the sensor

at balance are $\frac{V_1}{2}$ and $V_2/2$, respectively. The average input power P_{av} is equal to the change in dc power:

$$P_{av} = \frac{V_1^2}{4R} - \frac{V_2^2}{4R} = \frac{(V_1 - V_2)(V_1 + V_2)}{4R} \quad (13.12)$$

For any change in temperature if the voltage changes by ΔV , the change in RF power is $P_{av} + \Delta P = (V_1 + \Delta V)^2/4R - (V_2 + \Delta V)^2/4R$

$$\text{or } P_{av} + \Delta P = \frac{(V_1 - V_2)(V_1 - V_2 + 2\Delta V)}{4R} \quad (13.13)$$

Since $V_1 + V_2 \gg \Delta V$ in practice, $\Delta P \approx 0$. The meter responds to Eq. (13.13) to read microwave power P_{av} .

13.7.4 Thermocouple Sensor

A thermocouple is a junction of two dissimilar metals or semiconductors (n-type Si). It generates an emf when two ends are heated up differently by absorption of microwaves in a thin film tantalum-nitride resistive load deposited on a Si substrate which forms one electrode of the thermocouple as shown in Fig. 13.12. This emf is proportional to the incident microwave power to be measured.

Here C_2 is the RF bypass capacitor and C_1 is the input coupling capacitor or dc block. The emf generated in the parallel thermocouples are added to appear across C_2 . The output leads going to the dc voltmeter are at RF ground so that the output meter reads pure dc voltage proportional to the input microwave power.

For a square-wave modulated microwave signal the peak power can be calculated from the average power measured as

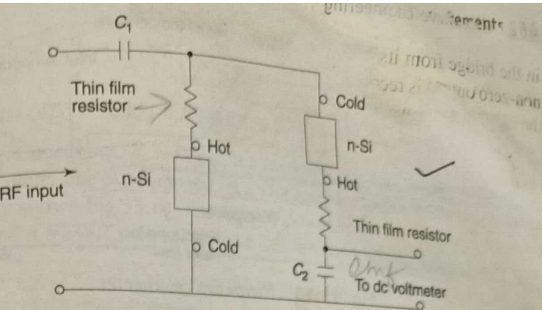


Fig. 13.12 Thermocouple power sensor

$$P_{peak} = \frac{P_{av} \times T}{\tau}$$

(13.14)

Where T is the time period and τ is the pulse width.

13.7.5 High Power Measurements by the Calorimetric Method

High power microwave measurements can be conveniently done by the calorimetric method which involves conversion of the microwave energy into heat, absorbing this heat in a fluid (usually water) and then measuring the temperature rise of the fluid as shown in Fig. 13.13. There are two types: one is the direct heating method and another is the indirect heating method. In the direct heating method, the rate of production of heat can be measured by observing the rise in the temperature of the dissipating medium. In indirect heating method, heat is transferred to another medium before measurement. In both the methods static calorimeter and circulating calorimeter are used.

Static calorimeters It consists of a 50 ohm coaxial cable which is filled by a dielectric load with a high hysteresis loss. The load has sufficient thermal isolation from its surrounding. The microwave power is dissipated in the load. The average power input is given by

$$P = \frac{4.187 m C_p T}{t} \text{ watts} \quad (13.15)$$

where

m = mass of the thermometric medium in gms

C_p = its specific heat in cal/gms

T = temperature rise in °C

t = time in sec.

Circulating calorimeters Here the calorimeter fluid (water) is constantly flowing through a water load. The heat introduced into the fluid makes exit temperature higher than the input temperature. Here average power

$$P = 4.187 v d C_p T \text{ Watts} \quad (13.16)$$

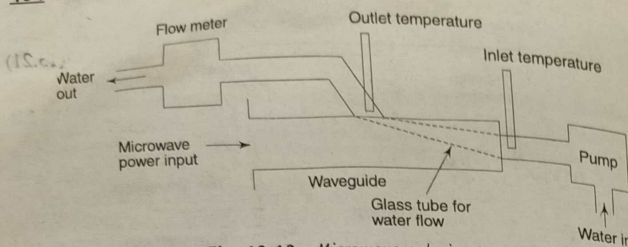


Fig. 13.13 Microwave calorimeter

where

 v = rate of flow of calorimeter fluid in cc/sec d = specific gravity of the fluid in gm/cc. T = temperature rise in °C C_p = specific heat in cal/gm

A disadvantage of calorimeter measurements is the thermal inertia caused by the lag between the application of microwave power and the parameter readings.

13.8 INSERTION LOSS AND ATTENUATION MEASUREMENTS

When a device or network is inserted in the transmission line, part P_r of the input signal power P_i is reflected from the input terminal and the remaining part $P_i - P_r$, which actually enters the network is attenuated due to the non-zero loss of the network. The output signal power P_0 is therefore less than P_i . Therefore, insertion loss is defined by the difference in the power arriving at the terminating load with and without the network in the circuit.

$$\text{Since, } \frac{P_0}{P_i} = \frac{P_i - P_r}{P_i} * \frac{P_0}{P_i - P_r} \quad (13.17)$$

or,

$$I.L. = RL + AL \quad (13.18)$$

$$10 \log \frac{P_0}{P_i} = 10 \log \left(1 - \frac{P_r}{P_i} \right) + 10 \log \left(\frac{P_0}{P_i - P_r} \right)$$

Insertion loss = reflection loss + attenuation loss
where, by definition

$$\text{Insertion loss (dB)} = 10 \log \frac{P_0}{P_i} \quad (13.19)$$

$$\begin{aligned} \text{Reflection loss (dB)} &= 10 \log \left(1 - \frac{P_r}{P_i} \right) \\ &= 10 \log (1 - |\Gamma|^2) \\ &= 10 \log \frac{4S}{(1+S)^2}; S = \frac{1-|\Gamma|}{1+|\Gamma|} \end{aligned} \quad (13.20)$$

$$\text{Attenuation loss (dB)} = 10 \log \left(\frac{P_0}{P_i - P_r} \right) \quad (13.21)$$

$$\text{Return loss (dB)} = 10 \log P_r/P_i = 20 \log |\Gamma| \quad (13.22)$$

For perfect matching, $P_r = 0$, and the insertion loss and the attenuation loss become the same. The experimental set up for insertion and the attenuation measurements are shown Fig. 13.14. The relative power levels are measured by using detectors and a VSWR meter. DC_1 and DC_2 are two identical directional couplers.

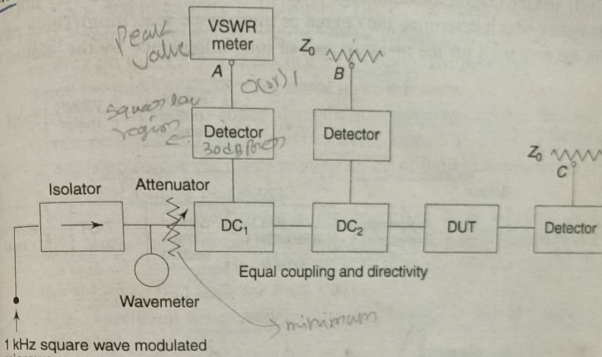


Fig. 13.14 Insertion loss and attenuation measurements

The following steps are involved for the insertion loss and attenuation measurements:

1. The microwave source is set to a suitable frequency and the 1 kHz square wave modulation level is adjusted for a peak reading on the VSWR meter at A with minimum input attenuation.
2. For a crystal detector to work in the square-law region the power level is adjusted to get a reading in the 30 dB range of the VSWR meter. The input power from port A is set to zero dB or 1.0 using gain control.
3. Frequency is read from the cavity frequency meter when a dip is observed in the VSWR meter.
4. Connecting matched load Z_0 to ports A and C and VSWR meter to port B, without disturbing any other set-up, the reading in the VSWR meter gives the ratio P_r/P_i , the return loss. The reflection loss $1 - (P_r/P_i)$ is calculated.
5. Now the input attenuator is adjusted to give an attenuation equal to the dB coupling of the directional coupler. The matched load is connected to ports A and B, and the VSWR meter to port C without disturbing any other set-up. The reading in the VSWR meter gives the ratio P_0/P_i , the insertion loss. Attenuation of the network under test can be determined by

subtracting the dB reflection loss from the dB insertion loss.

The main errors in this measurement are

1. P_r , P_0 and P_i may not all be capable of operating the crystal detector within its square-law region.
2. Both the directional couplers may not have the same characteristics.
3. There is some degree of mismatch between the various components in the set-up.

13.9 VSWR MEASUREMENTS

VSWR and the magnitude of voltage reflection coefficient Γ are very important parameters which determine the degree of impedance matching. These parameters are also used for the measurement of load impedance by the slotted line

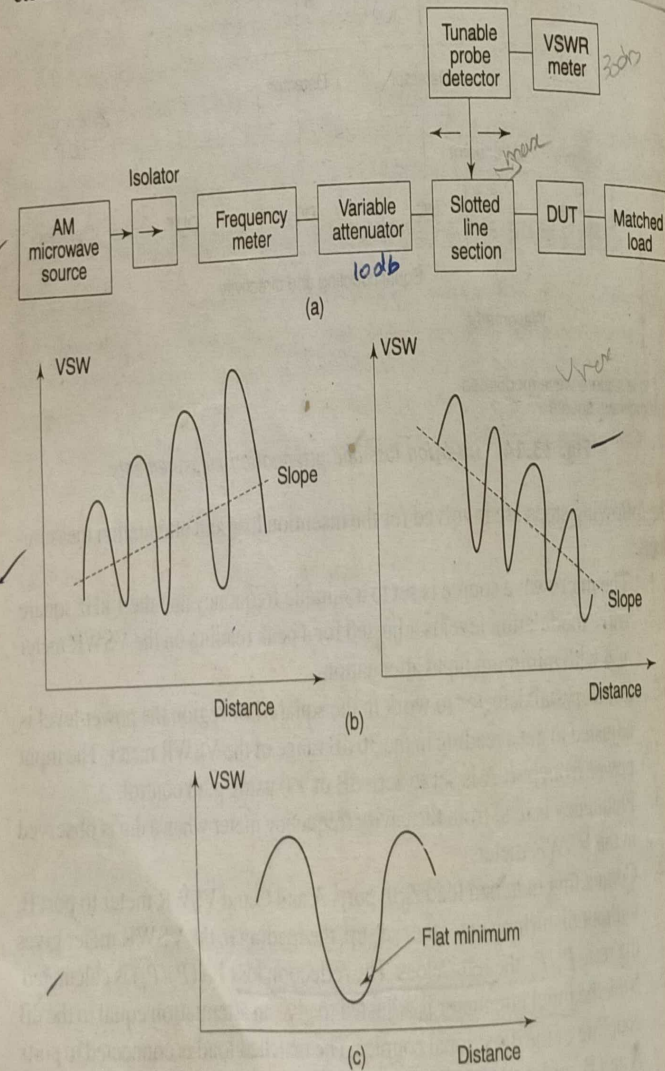


Fig. 13.15 Slotted line method of VSWR measurement (a) Basic experimental set-up (b) Slant pattern due to mechanical slope error (c) Flat minimum

method as shown in Fig. 13.15. When a load $Z_L \neq Z_0$ is connected to a transmission line, standing waves are produced. By inserting a slotted line system in the line, standing waves can be traced by moving the carriage with a tunable probe detector along the line. VSWR can be measured by detecting V_{\max} and V_{\min} in the VSWR meter : $S = V_{\max}/V_{\min}$.

13.9.1 Low VSWR ($S < 10$)

Low values of VSWR can be measured directly from the VSWR meter using the experimental set-up shown in Fig. 13.15 as follows.

1. The variable attenuator is adjusted to 10 dB. The microwave source is set to the required frequency. The 1 kHz modulation is adjusted for maximum reading on the VSWR meter in a 30 dB scale. The probe carriage stub is tuned for maximum detected signal in VSWR meter.
2. The probe carriage is slid along the non-radiating slot from the load end until a peak reading is obtained in VSWR meter. The meter's gain control is adjusted to get the meter reading at 1.0 or 0 dB corresponding to the position of voltage maximum.
3. The probe is moved towards the generator to an adjacent voltage minimum. The corresponding reading in VSWR meter directly gives the $VSWR = V_{\max}/V_{\min}$ on the top of SWR NORMAL scale for $1 \leq S \leq 4$ or on the EXPANDED scale for $1 \leq S \leq 1.33$.
4. The experiment is repeated for other frequencies as required to obtain a set of values of S vs f .
5. For VSWR between 3.2 and 10, a 10 dB lower RANGE should be selected and reading corresponding to V_{\min} position should be taken from the second VSWR NORMAL scale from the top.
6. For VSWR between 10 and 40, a 20 dB RANGE sensitivity increase is required and reading is taken from the top of VSWR NORMAL scale (1 to 4) at the voltage minimum and should be multiplied by 10 to obtain actual VSWR.
7. For VSWR between 32 and 100, a 30 dB lower RANGE must be selected and reading is taken from the second VSWR NORMAL scale (3.2 to 10) from the top at the voltage minimum. The reading should be multiplied by 10 to obtain actual VSWR.

The possible sources of error in this measurements are

1. V_{\max} and V_{\min} may not be measured in the square-law region of the crystal detector.
2. The probe thickness and depth of penetration may produce reflections in the line and also distortion in the field to be measured. Depth of penetration should be kept as small as possible otherwise values of VSWR measured would be lower than actual.
3. Mechanical slope between the slot geometry and probe movement may cause different values of VSWR for measurement at different locations along the slot (Fig. 13.15 b).

4. When $VSWR < 1.05$, the associated VSWR of connector produces significant error in VSWR measurement. Very good low VSWR (< 1.01) connectors should be used for very low VSWR measurements.
5. If the modulating 1 kHz signal is not a perfect square-wave, the microwaves will be frequency modulated and at each frequency there will be a different set of standing waves. This causes reduction in the sharpness of voltage minima and there may be error in the reading of minimum position as shown in Fig. 13.15 (c).
6. Any harmonics and spurious signals from the source may be tuned by the probe to cause measurement error.
7. A residual VSWR of slotted line arises due to mismatch impedance between the slotted line and the main line as explained in Fig. 13.16. Let

ρ_L = Actual load reflection coefficient

ρ_s = Slotted line reflection coefficient on main line

E_i = Incident electric field at any point on the main line

E_L = Reflected electric field from the load

E_s = Reflected electric field on the main line because of slotted line

Then, the total reflected field at a point = $|E_s \pm E_L|$. The maximum and minimum VSWR and reflection coefficients on the main line are

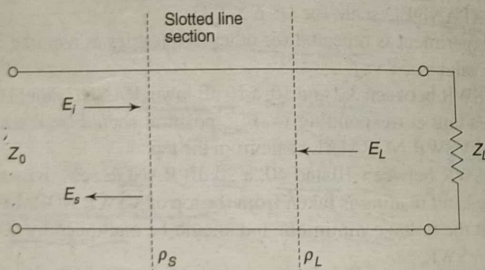


Fig. 13.16 Residual VSWR of slotted line

$$S_{\max} = \frac{E_i + (E_s + E_L)}{E_i - (E_s + E_L)} \quad (13.23)$$

$$S_{\min} = \frac{E_i + (E_s - E_L)}{E_i - (E_s - E_L)} \quad (13.24)$$

$$\rho_{\max} = \frac{S_{\max} - 1}{S_{\max} + 1} = |\rho_L| + |\rho_s| \quad (13.25)$$

$$\rho_{\min} = \frac{S_{\min} - 1}{S_{\min} + 1} = |\rho_L| - |\rho_s| \quad (13.26)$$

Microwave Measurements 469
The above equations can be solved for ρ_L and ρ_s from the measurements of S_{\max} and S_{\min} on the line. Then the residual VSWR.

$$S_s = \frac{1 + |\rho_s|}{1 - |\rho_s|} \quad (13.27)$$

13.9.2 High VSWR ($S > 10$)

For high VSWR, the difference of power at voltage maximum and voltage minimum is large, so it would be difficult to remain on the detector's square-law region at maximum positions when the diode current may exceed $20 \mu A$. Therefore, VSWR measurement with a VSWR meter calibrated on a square-law basis ($I = kV^2$) will be inaccurate. Hence double minimum method as shown in Fig. 13.17 is used where measurements are carried out at two positions around a voltage minimum point. The theory of this method can be established as follows. Let the ratio of line voltage near a minimum and the voltage at the minimum be

$$r_n = \frac{|V(x)|}{|V_{\min}|} \quad (13.28)$$

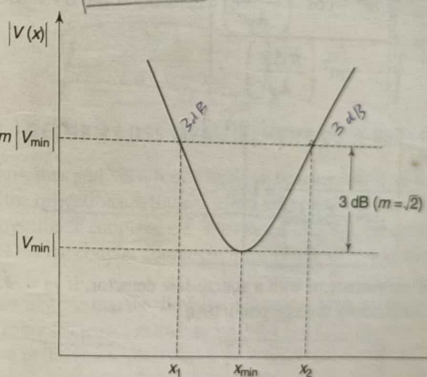


Fig. 13.17 Double minimum method

For a load reflection coefficient $\Gamma = \rho e^{j\phi}$. The line voltage at a distance x from the load end is

$$|V(x)| = |V_{\text{inc}}| |1 + \rho e^{j(\phi - 2\beta x)}|$$

$$|V(x)| = |V_{\text{inc}}| [1 + 2\rho \cos(\phi - 2\beta x) + \rho^2]^{1/2} \quad (13.29)$$

At the voltage minimum

$$|V_{\min}| = |V_{\text{inc}}| (1 - \rho) \text{ at } x = x_{\min} \quad (13.30)$$

If x_1 and x_2 are two points around x_{\min} where $|V(x_1)| = |V(x_2)| = m|V_{\min}|$,

$$m = \frac{|V(x_1)|}{|V_{\min}|} = \frac{[1 + 2\rho \cos(\phi - 2\beta x_1) + \rho^2]^{1/2}}{1 - \rho} \quad (13.31)$$

By substituting $\rho = (S-1)/(S+1)$, VSWR can be expressed as

$$S = \frac{\left[m^2 - \cos^2 \left(\frac{2\pi(x_1 - x_{\min})}{\lambda_g} \right) \right]^{1/2}}{\sin \left[2\pi(x_1 - x_{\min}) \right]} \quad (13.32)$$

where $\beta = 2\pi/\lambda_g$ and λ_g is the guide wavelength.

If x_1 is the point in the vicinity of x_{\min} ,

$$\Delta x = 2(x_1 - x_{\min}) \quad (13.33)$$

and

$$S = \sqrt{\frac{m^2 - \cos^2 \left(\frac{\pi \Delta x}{\lambda_g} \right)}{\sin^2 \left(\frac{\pi \Delta x}{\lambda_g} \right)}} \\ = \sqrt{\left[\frac{m^2 - 1}{\sin^2 \left(\frac{\pi \Delta x}{\lambda_g} \right)} + 1 \right]}^{1/2} \quad (13.34)$$

For convenience of measurement with a square-law detector, if $m = \sqrt{2}$ is selected, where x_1 is 3 dB above the x_{\min} point, then

$$S = \sqrt{\left[\frac{2-1}{\sin^2 \left(\frac{\pi \Delta x}{\lambda_g} \right)} + 1 \right]} \\ = \sqrt{1 + \operatorname{cosec}^2 \left(\frac{\pi \Delta x}{\lambda_g} \right)} \quad (13.35)$$

If $\pi \Delta x \ll \lambda_g$,

$$S \approx \operatorname{cosec} \left(\frac{\pi \Delta x}{\lambda_g} \right)$$

$$= \frac{1}{\sin \left(\frac{\pi \Delta x}{\lambda_g} \right)}$$

$$\approx \frac{\lambda_g}{\pi \Delta x}$$

$$(13.36)$$

where $\Delta x = x_2 - x_1$. Thus high VSWR can be measured by observing the distance between two successive minima to find λ_g and distance Δx between two 3 dB points on both sides of V_{\min} .

The method follows the steps given below.

1. The probe is moved to a voltage minimum and the probe depth and gain control is adjusted to read 3 dB in the VSWR meter.
2. The probe is moved slightly on either side of the minimum to read 0 dB in the meter. This position x_1 is noted. The probe is then moved to the other side of the minimum to read 0 dB again at x_2 .
3. By moving the probe between two successive minima a distance equal to $\lambda_g/2$ is found to determine the guide wavelength λ_g .
4. High VSWR is calculated from

$$S = \frac{\lambda_g}{\pi(x_1 - x_2)} \quad (13.37)$$

13.10 RETURN LOSS MEASUREMENT BY A REFLECTOMETER

The return loss and VSWR of a load can be determined by measuring the magnitude of the reflection coefficient with a reflectometer, a set-up in which two identical directional couplers are connected opposite to each other as shown in Fig. 13.18. One coupler couples to the forward wave and the other to the reverse wave.

Let us assume that the directional couplers have infinite directivity, a voltage coupling coefficient C , main line VSWR 1 and the detectors have constant impedance and perfect matching to the line. When a unit input amplitude is fed to port 1, voltages at ports 4 and 2 are, respectively,

$$b_4 = C \quad (13.38)$$

$$b_2 = (1 - C^2)^{1/2} \quad (13.39)$$

Incident voltage at port 2 is reflected by the load under test. If Γ_L is the reflection coefficient, the reflected wave amplitude at port 2 is

$$a_2 = (1 - C^2)^{1/2} |\Gamma_L| \quad (13.40)$$

This will be coupled to port 3 to produce a voltage of

$$b_3 = (1 - C^2)^{1/2} C |\Gamma_L| \quad (13.41)$$

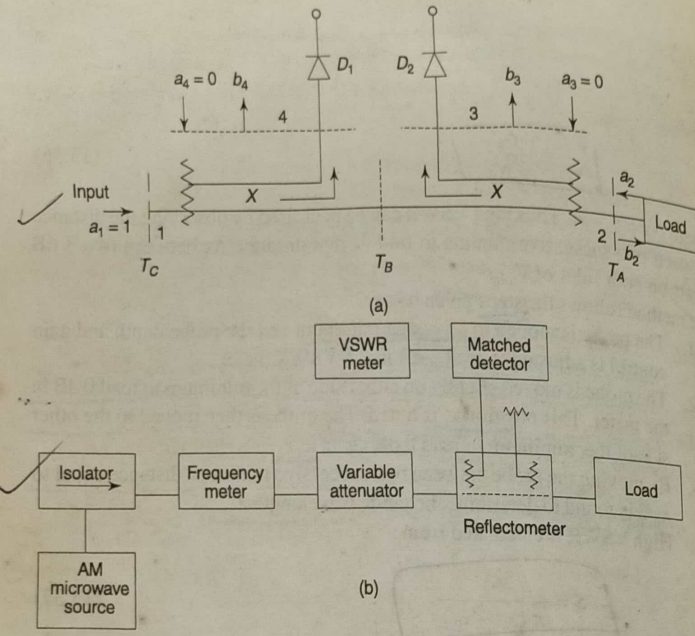


Fig. 13.18 (a) Reflectometer (b) Experimental set-up for a reflectometer

$$\text{Then } |b_3/b_4| = (1 - C^2)^{1/2} |\Gamma_L| = K |\Gamma_L| \quad (13.42)$$

If coupling is extremely small i.e. $C \ll 1$, $K \approx 1$. Therefore,

$$|b_3/b_4| = |\Gamma_L|. \quad (13.43)$$

Thus, knowing the voltage ratio between ports 3 and 4, the reflection coefficient and hence VSWR and return loss can be determined from the following relations.

$$S = \text{VSWR} = \frac{1 + |\Gamma_L|}{1 - |\Gamma_L|} \quad (13.44)$$

$$\text{Return loss} = -20 \log |\Gamma_L| \quad (13.45)$$

The experiment is conducted first by terminating port 2 with a short and adjusting the output of the detector D_1 at port 4 to unity in VSWR meter while detector D_2 at port 3 is matched terminated. VSWR meter and match load at D_1 and D_2 are now interchanged. The output of the port 3 is noted which should ideally be equal to the output from port 4. Without disturbing the VSWR meter adjustment, the unknown load is connected at port 2 by replacing the short and the output at port 3 is noted to obtain $1/|\Gamma_L|$ directly from the VSWR meter.

This method is well suited for loads having low VSWR. The major source of error in this method is that the instability of the signal source causes a change in signal power level during measurement of input and reflected signal levels at different instants of time. Non-ideal directional couplers and detectors are also sources of error.

13.11 IMPEDANCE MEASUREMENT

Since impedance is a complex quantity, both amplitude and phase of the test signal are required to be measured. The following techniques are commonly employed for such measurements:

13.11.1 Slotted Line Method

The complex impedance Z_L of a load can be measured by measuring the phase angle ϕ_L of the complex reflection coefficient Γ_L from the distance of first voltage standing wave minimum d_{\min} and the magnitude of the same from the VSWR. S. The following relations are important for the computation of Z_L .

$$Z_L = Z_0 \frac{1 + \Gamma_L}{1 - \Gamma_L} \quad (13.46)$$

$$\Gamma_L = \rho_L e^{j\phi_L} \quad (13.47)$$

$$S = (1 + \rho_L)/(1 - \rho_L) \quad (13.48)$$

$$\phi_L = 2\beta d_{\min} - \pi \quad (13.49)$$

$$\beta = 2\pi/\lambda_g \quad (13.50)$$

$$\lambda_g = 2 \times \text{distance between two successive minima.}$$

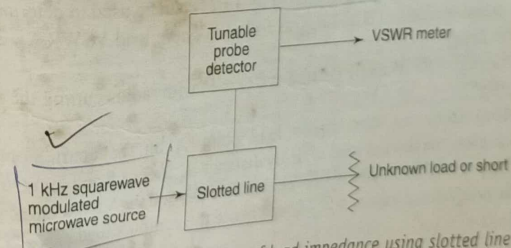


Fig. 13.19 Determination of load impedance using slotted line

The method of using slotted line to determine an unknown impedance is explained in Fig. 13.19. The steps for measurement are summarized below.

1. Measure the load VSWR to find ρ_L from Eq. 13.48.
2. Measure the distance d between two successive voltage minima to find $\beta = 2d/\lambda_g$
3. Measure the distance d_{\min} of the first voltage minimum from the load plane towards generator in the following manner.

Since it may not be possible to reach the first d_{\min} by the probe close to the load directly using slotted line, an equivalent load reference plane on the slotted line is established by means of a short circuit at the load reference plane where a voltage minimum now occurs. Since a series of minima are produced on the slotted line at intervals of $\lambda_g/2$, the load reference plane can be shifted to a convenient minimum position near the centre of the slotted line as shown in Fig. 13.20. The d_{\min} can then be measured by observing the first minimum from this shifted reference plane when the load replaces the reference short.

4. Phase angle ϕ_L of the load is calculated from Eq. 13.49 and hence $\Gamma_L = p_L e^{j\phi_L}$ is found.
5. The unknown impedance Z_L is then calculated from Eq. 13.46.)

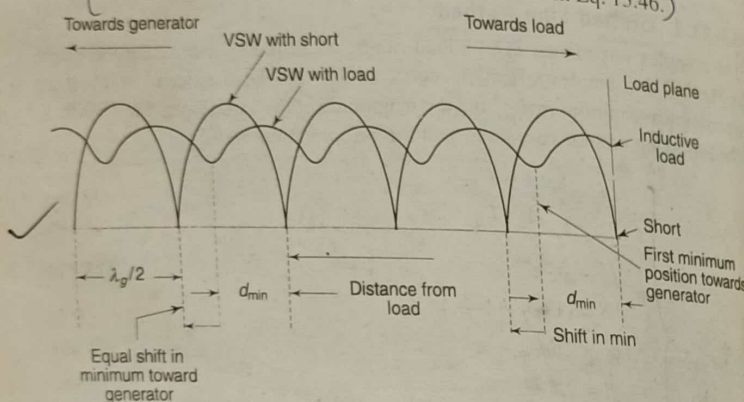


Fig. 13.20 Determination of d_{\min}

To ease the calculation, Smith chart (Fig. 13.21) can be used to determine Z_L from the measurements of S and d_{\min} as follows, where load VSWR $S = 2$, and $d_{\min}/\lambda_g = 0.2$, say.

1. Draw the VSWR circle centred at 0 ($r = 1$) with radius cutting the r -axis at $S = 2$.
2. Move from the short circuit load point A on the chart along the wavelengths toward load scale by distance d_{\min}/λ_g to B and join OB .
3. The point of intersection between the line OB and the VSWR circle gives the normalised load $z_L = Z_L/Z_0$ and hence the complex load $Z_L = Z_0(1.0 + j0.7)$.

13.11.2 Impedance Measurement of Reactive Discontinuity

The impedance of a shunt reactive discontinuity, such as a post or windows or a step in a microwave transmission line, can be measured using the slotted line method from the measurement of line VSWR and the distance of first voltage minimum from the discontinuity plane as follows.

Let jX be the reactance of the discontinuity at load distance point $d = 0$. The line is terminated by a matched load R_0 at $d = 0$. The total impedance of the combination is

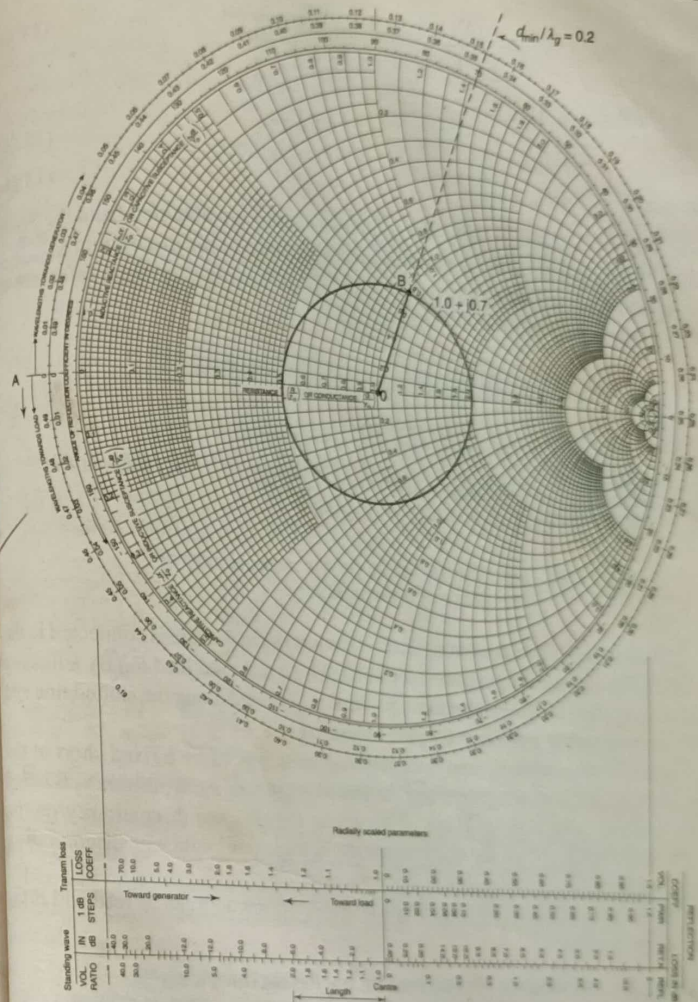


Fig. 13.21 Smith chart for Z_L measurement

$$Z_L = \frac{R_0 \cdot j X}{R_0 + j X} \quad (13.51)$$

The normalised value

$$\frac{Z_L}{R_0} = \frac{j X}{R_0 + j X} = \frac{X^2}{R_0^2 + X^2} + j \frac{X R_0}{R_0^2 + X^2} = x + jy, \text{ say} \quad (13.52)$$

where, $x = \frac{X^2}{R_0^2 + X^2}, y = j \frac{X R_0}{R_0^2 + X^2}$ (13.53)

with X unknown. Here we see that

$$X/R_0 = x/y$$

or, $B/G_0 = y/x$ (13.54)

where $B = 1/X$ and $G_0 = 1/R_0$. The values of x and y are obtained from the Smith chart to find the value of the normalised susceptance of the discontinuity.

The procedure of measurement follows the following steps with reference to the experimental set-up shown in Fig.13.22.

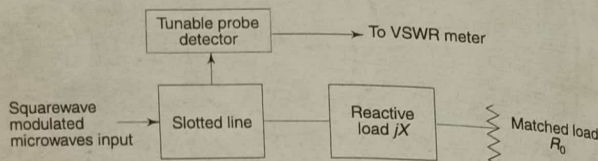


Fig. 13.22 Experimental set up for the measurement of impedance of a discontinuity

Discontinuity such as a tuning screw or windows in the line is connected to the slotted line and the output port is terminated by a matched load R_0 . By adjusting the tuning stub, a voltage minimum position, x_1 , is noted along the slotted line and the corresponding VSWR and λ_g are measured.

Next the discontinuity and matched load are replaced by a fixed short at the point of the discontinuity position. The first voltage minimum position x_2 is noted towards the load from x_1 . Thus x_2 translates the plane of discontinuity on the slotted line scale so that the distance of first voltage minimum with discontinuity and matched load termination is $d_{\min} = (x_1 - x_2)$.

By locating d_{\min}/λ_g , S on the Smith chart, $Z_L/R_0 = x + jy$ can be read and $B/G_0 = y/x$ is calculated.

13.11.3 Impedance Measurement by Reflectometer

The reflectometer arrangement shown in Fig.13.18(a) cannot have ideal conditions of infinite directivity, constant impedance detectors and perfect impedance matching. When the unknown impedance is connected to the output port, the ratio of the signal amplitudes at ports 3 and 4 is, in general

$$\left| \frac{b_3}{b_4} \right| = \frac{A \Gamma_L + B}{C \Gamma_L + D} \quad (13.56)$$

where A, B, C and D are functions of the S -parameters of the four ports formed by the reflectometer. By using two tuners T_A and T_B , a movable short, and a sliding load of low VSWR (< 1.02), the above ideal conditions could be achieved as shown in Fig.13.23.

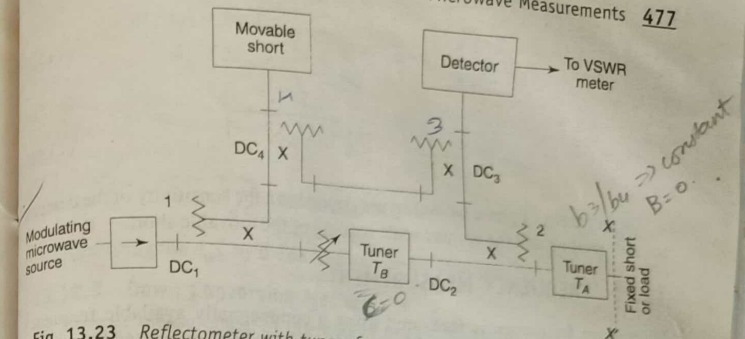


Fig. 13.23 Reflectometer with tuners for amplitude and phase measurements

Tuner T_A is adjusted to make $|b_3/b_4|$ constant while the phase of Γ_L is varied by changing the position of a sliding load at port 4. This makes $B=0$. The tuner T_B is adjusted to make $|b_3/b_4|$ constant as the phase of Γ_L is varied by changing the position of a sliding short at port 4, then $C=0$. Hence

$$\left| \frac{b_3}{b_4} \right| = \left| \frac{A}{D} \right| |\Gamma_L| = K |\Gamma_L| \quad (13.57)$$

or,

$$|\Gamma_L| = \frac{1}{K} \left| \frac{b_3}{b_4} \right| \quad (13.58)$$

For a given bridge, K is determined by noting $|b_3/b_4|$ using a fixed short of known reflection coefficient of -1 at port 4 and, therefore, by measuring $|b_3/b_4|$, the magnitude of reflection coefficient of any load at port 2 can be determined.

In order to measure the phase of the load reflection coefficient, four identical directional coupler reflectometer can be used as shown in Fig.13.23. The procedure of phase measurements is as follows:

- First a fixed short is placed at XX' plane of the precession waveguide section at port 2. The movable short at port 4 and the attenuator are adjusted to obtain null in the detector output at port 3.
- The fixed short at port 2 is replaced by the test load and a shift x of the movable short at port 4 is measured to obtain null in the detector output at port 3.

The phase of Γ_L is then given by

$$\phi_L = \frac{2\pi\Delta x}{\lambda_g} \quad (13.59)$$

Thus

$$\Gamma_L = K \left| \frac{b_3}{b_4} \right| e^{j\phi_L} \quad (13.60)$$

and

$$Z_L = Z_0 \frac{1 - \Gamma_L}{1 + \Gamma_L} \quad (13.61)$$

The accuracy of phase measurement depends on the sensitivity of the detector for null reading and the vernier scale reading of the movable short.

13.12 FREQUENCY MEASUREMENT

Microwave frequency is measured using a commercially available frequency counter and cavity wavemeter. The frequency also can be computed from measured guide wavelength in a voltage standing wave pattern along a short circuited line by using a slotted line.

13.12.1 Wavemeter Method

A typical wavemeter is a cylindrical cavity with a variable short circuit termination which changes the resonance frequency of the cavity by changing the cavity length. As discussed in Section 7.5, TE_{011} mode is most suitable for wave meter because of its higher Q and absence of axial current. Since this is higher order mode, possibility of generation of lower order modes exists. Hence for practical purposes dominant TM_{010} mode is used in wavemeter applications. Wavemeter axis is placed perpendicular to the broad wall of the waveguide and coupled by means of a hole in the narrow wall as shown in Fig. 13.24. This excites TM_{010} mode in the cavity due to the magnetic field coupling. A block of absorbing material (Polytron) placed at the back of the tuning plunger prevents oscillation on top of it. Thus the cavity resonates at different frequencies for different plunger positions. The tuning can be calibrated in terms of frequency by known frequency input signals and observing the dip in the display unit (power meter) connected at the output side of waveguide. The accuracy of such a wavemeter is in the range of 1% to 0.005% for available Q of 1,000–50,000, respectively. Since the power is absorbed in the wavemeter at resonance this is called absorption type wavemeter.

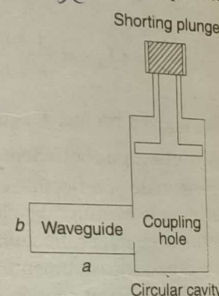


Fig. 13.24 Wavemeter method of frequency measurements

13.12.2 Slotted Line Method

Since the distance d_{min} between two successive minima of voltage standing wave pattern in a short circuited line is half wavelength $\lambda_g/2$, frequency can be determined from the relations

$$f(\text{GHz}) = 30/\lambda_0 \text{ (cm)} \quad (13.62)$$

$$\lambda_g = 2d_{min} \quad (13.63)$$

$$= \frac{\lambda_0}{[1 - (\lambda_0/2a)^2]^{1/2}} \text{ for waveguide} \quad (13.64)$$

$$= \frac{\lambda_0}{\sqrt{\epsilon_r}} \text{ for coaxial line} \quad (13.65)$$

and measuring the d_{min} by the slotted line probe carriage.

13.12.3 Down Conversion Method

An accurate measurement of microwave frequency can be done by means of a heterodyne converter. A heterodyne converter (Fig. 13.25) down converts the unknown frequency f_x by mixing with an accurately known frequency f_a , such that the difference $f_x - f_a = f_{IF}$ is amplified and measured by the counter. The frequency f_a is selected by first multiplying a local oscillator frequency (known) to a convenient frequency f_1 and then passing it through a harmonic generator that produces a series of harmonics of f_1 . The appropriate harmonic $nf_1 = f_a$ is selected by the tuning cavity such that f_a can be added with f_{IF} and display f_x (counter reading $+f_a$), the unknown frequency. In practice, the system starts with $n = 1$ and the filter frequency is selected by a feed back mechanism from IF stage until an IF frequency in the proper range is present. Typically, $f_1 = 100$ to 500 MHz for a range of f_x up to 20 GHz. For better accuracy a low noise oscillator and noiseless multiplier are to be selected.

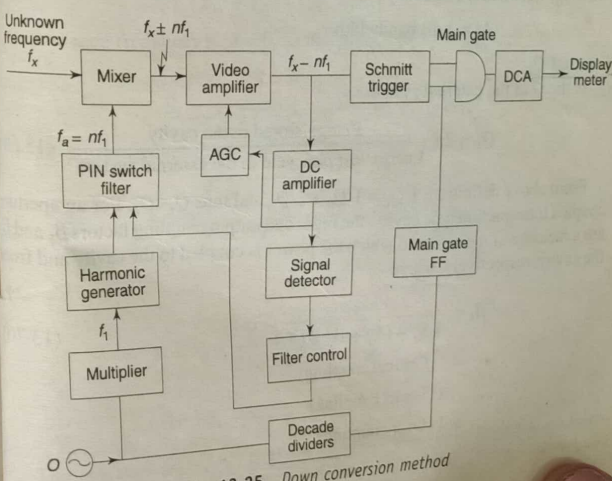


Fig. 13.25 Down conversion method

13.13 MEASUREMENT OF CAVITY Q

A difficult measurement at microwave frequencies is the accurate measurement of Q of a high Q cavity. This is due to the fact that the 3dB bandwidth of the cavity response curve is a very small fraction of the resonance frequency. Moreover, the cavity has to be loaded during such measurements and Q becomes lower. There are three definitions of Q , connected to the associated circuit which are summarized below.

Unloaded Q_0

$$Q_0 = 2\pi \frac{\text{Energy stored in the cavity}}{\text{Energy lost per cycle in the cavity}} \quad (13.66)$$

Q_0 is selectivity factor of the cavity, dependent on the geometrical portion of the cavity. The expressions for Q_0 of several cavities are given in Section 7.5 in terms of their dimensions and mode numbers.

Loaded Q_L

$$Q_L = 2\pi \frac{\text{Energy stored in the cavity}}{\text{Energy lost per cycle in the cavity} + \text{Energy lost per cycle in the external system}} \quad (13.67)$$

Q_L is the Q of the entire system, including all sources of energy loss.

Q_L can be determined by the formula

$$Q_L = f_0/\Delta f \quad (13.68)$$

where f_0 = resonance frequency

Δf = 3 dB bandwidth

External Q_E

Q_E is the Q of the external system.

$$Q_E = 2\pi \frac{\text{Energy stored in the cavity}}{\text{Energy lost per cycle in the external system}} \quad (13.69)$$

From above definition, $1/Q_L = 1/Q_0 + 1/Q_E$ and thus $Q_L < Q_0$. For an aperture coupled transmission type cavity, the input and output coupling factors β_1 and β_2 are a measure of the extent to which the power is coupled to the cavity and from the cavity, respectively, where

$$\begin{aligned} \beta_1 &= \frac{4}{4S_0 - (S_0 + 1)^2 T(f_0)} \quad (13.70) \\ &= 1 \text{ (Critical coupling)} \\ &< 1 \text{ (Under coupling)} \\ &> 1 \text{ (Over coupling)} \end{aligned}$$

and

$$\beta_2 = \beta_1 S_0 - 1 \quad (13.71)$$

$$Q_0 = Q_L(1 + \beta_1 + \beta_2) \quad (13.72)$$

Here S_0 = VSWR at the resonance frequency f_0 .

$$T(f_0) = P_{\text{out}}/P_{\text{in}} \quad (13.73)$$

= Transmission loss at the resonance frequency f_0 .

Measurement of both the transmission loss $T(f_0)$ and VSWR S_0 at resonance gives the data needed for calculating β_1 and β_2 and determining Q_0 . A brief description of several methods of measurement of Q is given below.

13.13.1 Slotted Line Measurement of Q

A slotted line may be used to measure the Q of a reflection type cavity which is normally used in a microwave tube, through pure VSWR measurements or through measurement of the shift in position of a standing wave minimum as the generator frequency is varied. Here the VSWR in the line that feeds the cavity is uniquely related to the variation in amplitude of the cavity input reflection coefficient and the shift of minimum is related to the variation of phase angle of the complex voltage reflection coefficient. The measurement set-up is shown in Fig.13.26. The half-power frequency is found directly from the VSWR measurement, where the equivalent resonator reactance is assumed to be equal in magnitude to the equivalent resonator resistance. If $Z_{\text{in}} = R + jX$ is the input impedance in the vicinity of resonance of the cavity, VSWR

$$S = \frac{|Z_{\text{in}} + Z_0| + |Z_{\text{in}} - Z_0|}{|Z_{\text{in}} + Z_0| - |Z_{\text{in}} - Z_0|} \quad (13.74)$$

At resonance frequency f_0 , $X = 0$, so that minimum VSWR S_0 is

$$\begin{aligned} S_0 &= R/Z_0, \text{ if } R > Z_0 \\ &= Z_0/R, \text{ if } R < Z_0 \end{aligned} \quad (13.75)$$

At half-power frequencies f_1 and f_2 of the unloaded cavity, $X = R$, so that

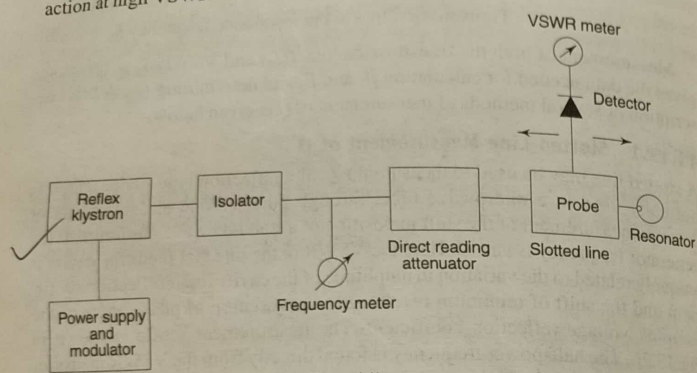
$$S_1 = \frac{\sqrt{[(R + Z_0)^2 + R^2]} + \sqrt{[(R - Z_0)^2 + R^2]}}{\sqrt{[(R + Z_0)^2 + R^2]} - \sqrt{[(R - Z_0)^2 + R^2]}} \quad (13.76)$$

or,

$$\begin{aligned} S_1 &= S_0 + \frac{1}{2S_0} + \sqrt{\left(S_0^2 + \frac{1}{4S_0^2}\right)} ; R > Z_0 \\ &= 1/S_0 + S_0/2 + \sqrt{(1/S_0^2 + S_0^2/4)} ; R < Z_0 \end{aligned} \quad (13.77)$$

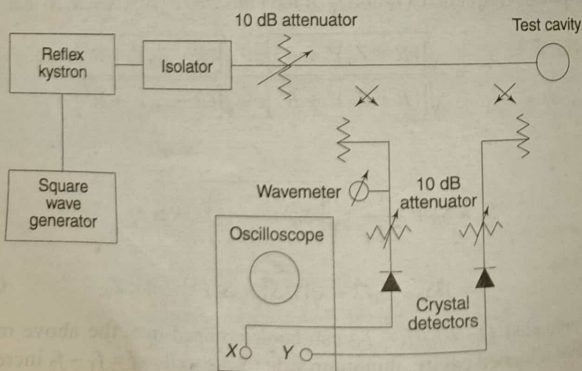
The unloaded $Q_0 = f_0/(f_1 - f_2)$ can be determined from the above measurements. For a loaded cavity, minimum value S_0 as well as $f = f_1 - f_2$ increase and

this results in a lower value of Q . The accuracy of measurement lies on the half-power VSWR and half-power bandwidth. In this method the measurement errors include the departure from square-law behaviours of the probe detector, frequency instability of the source, generator mismatch, probe and generator interaction at high VSWR.

Fig. 13.26 Slotted line measurement of Q

13.13.2 Reflectometer Method of Measurement of Q

This method is suited for a reflection cavity and provides oscilloscope presentation by a swept microwave source. The method determines the magnitude of voltage reflection coefficient Γ at resonance, at half-power points and at a point far away from resonance $\Gamma \approx 1$. A schematic of the experimental set-up is shown in Fig. 13.27. The total errors in the measurement depends essentially on the accuracy of measuring the bandwidth and in setting half-power level for the reflection coefficient. The errors in half-power point for the reflection coefficient depend on the imperfect directivity of directional couplers and instability of the source frequency.

Fig. 13.27 Reflectometer method of measurement of Q

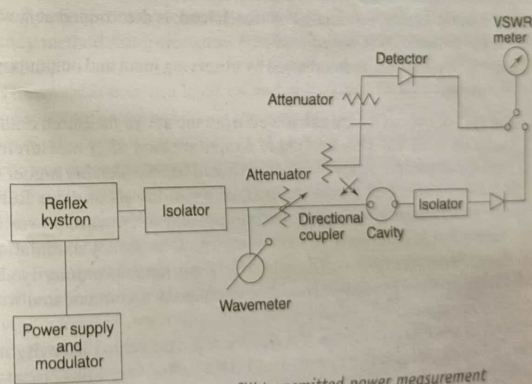
13.13.3 Q From Transmitted Power Measurement

This method uses the power transmitted through a cavity as a function of frequency, for measuring loaded Q . This method can be used for both transmission and the reflection type cavities. The transmission method has the advantage that the loaded Q can be measured directly regardless of the existence of coupling losses. However, this method cannot yield the unloaded Q without a number of additional measurements. The basic procedure can be carried out in several different ways as discussed below.

There are three main sources of error in the transmission method of Q measurement. The first relates to a possible mismatch of the generator and load between which the cavity is inserted. The second relates to the most important error that arises in measuring the bandwidth of the cavity response curve. Third is that due to the inaccuracies in relative power measurements, caused either by imperfect calibration of attenuators or power meters, or imperfect square-law response of detectors, errors in the readings of meters and attenuator dials, or by both calibration and reading errors.

(i) CW measurement

The CW measurement set-up is illustrated in Fig. 13.28. The transmitted CW power can be monitored with a power meter. Alternatively, the RF signal may be square-wave modulated and a tuned amplifier or a VSWR meter may be used at the output of the square-law crystal detector to indicate the transmitted powers at resonance frequency f_0 and half power points $f_0 \pm \Delta f/2$. Q is calculated from $f_0/\Delta f$. To avoid errors due to non square-law response from the crystal at different power levels, a calibrated attenuator may be used for determining the half-power frequencies by keeping input power level same in all measurements.

Fig. 13.28 Q from CW transmitted power measurement

(ii) Swept frequency measurement of Q A swept frequency technique (Fig. 13.29) requiring less frequency stability of the RF source than the above

procedures, provides simultaneous display of two oscilloscope traces, one proportional to the incident power, the other to the power transmitted through the cavity. The method uses a pair of matched crystal detectors of the same response law over the power and frequency range of the measurements. The wave meter measures the resonance frequency f_0 and the half-power frequency from the dip in the input response curve at the output peak and half-power points, respectively, to yield loaded Q_L .

The procedure of measurement is as follows.

1. A linear sweep (saw-tooth wave) voltage is applied to the repeller of the reflex klystron so that a FM microwave signal is produced. Since the expected cavity bandwidth is much smaller than the frequency swing of FM signal, we can assume constant input voltage to the cavity at different frequencies around the resonance frequency of the cavity. Applying voltage to the triggering input of a double beam CRO from the same sweep generator, a response of the cavity is obtained in Y_2 beam.

To determine the resonant frequency and 3 dB bandwidth a marker trace is generated by applying a detected signal from the auxiliary arm of the directional coupler to Y_1 beam on the CRO. This represents the klystron power output mode characteristics.

By tuning the klystron frequency, cavity response is maximised and cavity peak response and peak of the klystron mode is made coincident. The frequency meter is adjusted to obtain a dip at the peak of cavity response. This indicates resonant frequency of the cavity. The flat top of the klystron mode curve is now adjusted to 3 dB point of the cavity response and the frequency bandwidth is noted by observing frequency meter readings corresponding to the dip in the response at 3 dB points.

2. VSWR of the cavity, terminated by match load, is determined at f_0 with a slotted line and VSWR meter.
3. Transmission loss at f_0 is determined by observing input and output powers of the cavity.

The α_0 and Q_L of the cavity are calculated from the above measured data and using Eqns. 13.68 – 13.73. This method is a rapid method of Q measurement. Obviously the Q_L of the frequency meter used should be considerably higher than that of the cavity under test to set the marker positions accurately. Reflex-klystrons are widely used as sources of swept frequency microwave power. The electronic tuning range of reflex klystron within which frequency modulation is possible, is comparatively narrow. Thus at 10 GHz this range is ordinarily about 10–15 MHz and the resonance curve should be completely accommodated within this frequency range.

A further limitation of measurement is that the input power to the cavity must be maintained constant within the cavity band. This limits very low Q measurement by this technique.

Accuracy of the measurement depends on the measurement of very low bandwidth. Therefore, resolution of the frequency meters should be very high. Eye estimation in measuring bandwidth also introduces some error. Errors can be reduced by taking the average of several observations.

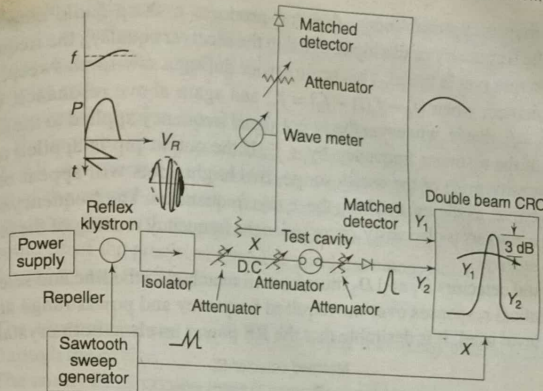


Fig. 13.29 Swept frequency measurement of Q

(iii) Swept frequency measurement of Q using electronic frequency marker
Bandwidth measurement accuracy is the most important factor in high Q measurement. Ordinarily when the test cavity Q is not very high, a high Q cavity wavemeter may be used to measure half-power frequencies. A cavity operating at 10 GHz with a high Q of 10,000 has a bandwidth of 1 MHz. It is difficult to adjust the microwave oscillator for such a small frequency difference. Moreover, it is difficult to measure this frequency difference since standard cavity wavemeters have smallest scale division of 1 to 5 MHz.

For very accurate measurement of high Q in a laboratory set-up swept frequency method using electronic frequency marker can be employed as shown in Fig. 13.30.

The swept source is a klystron and is shown to be saw-tooth modulated. The same saw-tooth sweep is simultaneously applied to the horizontal input of a dual trace oscilloscope to give displays of incident and transmitted power versus frequency on the oscilloscope screen synchronously. Saw-tooth generates FM signal from the klystron with envelope variation in accordance with the klystron mode curve and the cavity response curve. Both the input and output signal of the cavity are detected by means of crystal detectors before being fed to the CRO. The markers are generated with the aid of an auxiliary frequency stable low frequency oscillator (~ 800 MHz) are combined in a harmonic crystal mixer which is connected to the input of a superheterodyne receiver. Harmonics of low frequency signal are mixed with the swept frequencies. Sum and difference frequencies produced in the mixer. The superhet receiver can respond only to the time varying produced in the mixer. The superhet receiver can respond only to the time varying

difference frequency component, $f_s(t)$ and produces a sharp audio output pip whenever the frequency of the input signal to the receiver equals f_r , the frequency to which the receiver is tuned. This occurs twice during a saw-tooth sweep, once below resonance, when $|f_0 - f_s(t) - f_r| = f_r$, and again above resonance, when $f_0 + f_s(t) - f_r = f_r$, that is, whenever the swept signal frequency applied to the cavity differs from the resonant frequency by $\pm f_r$. If the output pip is applied to the Z-axis (intensity grid) of the oscilloscope, two bright spots will appear on the resonance curve, as shown, marking these two frequencies. The frequency separation of the markers is obviously $2f_r$, or twice the frequency reading of the tuning dial of the receiver.

The crystal detectors D_1 and D_2 must be well matched to the line and selected to give identical responses over the required frequency and power range and at the power level used. It is desirable that the RF power levels at both crystals be

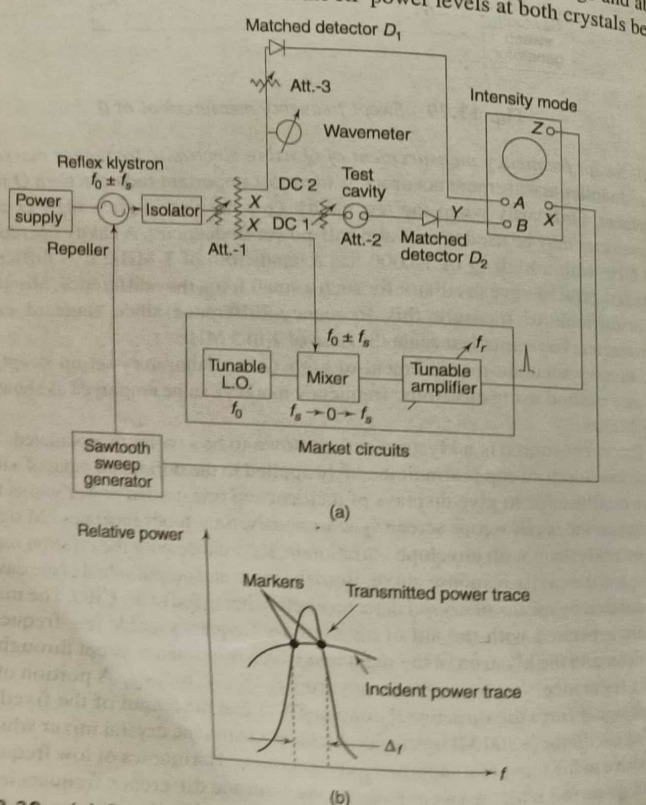


Fig. 13.30 (a) Swept frequency measurement of Q using electronic frequency markers (b) Input and output power traces

nearly the same. This makes it necessary that the sum of the attenuation in Att. 2 and the cavity insertion loss (in dB) in the transmitted power channel be approximately equal to the (dB) coupling loss and sum of the attenuations in the directional coupler arm.

The directional coupler should have high directivity in the frequency range of interest. The isolator should have at least 20 dB of isolation and VSWR better than 1.2. All the attenuators should have a good VSWR (<1.10). Broadband matching of the crystal detectors can be obtained by using well matched 10 dB fixed pads in tandem with the crystal mounts. The calibrated variable attenuator Att.-3 should be of the precision type. For good matching, isolators may be used before the cavity and the detector.

Checking crystals

1. The klystron is tuned to f_0 by observing maximum transmitted signal through the cavity.
 2. The cavity transmission trace B from D_2 should be centred with respect to the incident power trace A from D_1 .
 3. The dual trace oscilloscope vertical centering controls are adjusted so that the base lines of the two traces A and B coincide. During this adjustment, the RF power is completely removed.
 4. Attenuator Att.-3 is set to zero. Att-1 and 2 are adjusted so that the peak of the trace from D_2 just touches the trace from D_1 .
 5. The cavity is removed and Att-2 is adjusted so that the traces of the two crystals coincide.
 6. The coincident traces are checked by increasing the attenuation of Att-1 by approximately 6 dB. The two traces should remain coincident over this range. Otherwise, discrepancies between the two crystals are noted and later applied as a correction. The amount of the discrepancy can be determined by adjusting Att-3 starting with some initially inserted attenuation and observing the change in setting required to align both traces exactly.
 7. Steps 1–6 are repeated for a few frequencies in the neighborhood of f_0 .
- Measurement procedure*
1. When the cavity is removed from the test position, the RF frequency sweep is adjusted so as to cover a sufficiently large portion of the cavity resonance curve. Calibrated attenuators 2 and 3 are adjusted so that the incident and transmitted power traces coincide. Coincidence of baselines of the two traces for zero RF power signal is done previously.
 2. The test cavity is then inserted and the klystron repeller voltage is adjusted and it is tuned at resonance f_0 so that both the transmitted and incident power traces on the scope are centred. Att.-2 is adjusted so that the incident power trace touches the maximum power point of the transmitted power trace, corresponding to f_0 as shown in Fig. 13.31(b). The change in power of Att.-2 is the cavity transmission loss at resonance $T(f_0)$. Attenuation of Att.-3 is kept at 0 dB. Resonance frequency f_0 is observed by using of reaction wavemeter.

3. The incident power trace is lowered down by adding 3 dB attenuation with Att.-3.
4. The markers are placed at the points of intersection of the incident and transmitted power traces at the above setting of Att.-3 by tuning the superhet receiver. The tuning frequency f_r is noted to determine half-power bandwidth $\Delta f = 2f_r$.
5. Q_L is calculated from $f_0/2f_r$.
6. For the VSWR measurement, the klystron is square-wave modulated. A slotted line with a tunable probe detector is inserted at the input of the cavity and output is matched terminated. Detected signal from the slotted line is fed to a VSWR meter. VSWR S_1 are measured at frequencies around f_0 . Also S_0 at f_0 is determined.

The Q_0 is calculated from equation 13.68 – 13.73.

Accuracy of measurement

Advantages of swept frequency measurements of Q with frequency markers are

- Requires less frequency stability of the RF source
- Accurate measurement of bandwidth
- Measurement time is small.
- Q measurement by phase shift of modulation envelope of transmitted signal [8,9]

When a microwave signal of frequency f_0 is sine wave amplitude modulated at a frequency f_1 and applied to a transmission cavity having a resonant frequency f_0 , the modulation envelope of the transmitted signal will be delayed in phase with respect to that of the impressed signal by an angle

$$\theta = \tan^{-1}(2Q_L f_1/f_0) \quad (13.78)$$

If f_1 is made equal to $\Delta f/2$, where Δf = half-power bandwidth, and $\theta = 45^\circ$, then $Q_L = f_0/2f_1$. Since f_1 can be accurately known from the frequency calibration of the modulating generator, Δf and hence Q_L can be determined. When a sine wave amplitude modulated carrier wave is applied to a resonant circuit at its resonant frequency, its sidebands are symmetrically shifted in phase on transmission through the resonator, one sideband being advanced, the other delayed with respect to the input wave, as shown in Fig. 13.31. This results in the phase shift in the modulation envelope shown in Fig. 13.31(c), which may be measured by means of a phase meter. The advantages of this method are that it is capable of bandwidth measurements and the measurement is much less affected by frequency stability of the microwave generator. This follows from the fact that the phase shift of the modulation envelope of the transmitted wave is a maximum when the carrier is at the resonant frequency of the cavity.

The accuracy of measurement depends ultimately on the accuracy of the precision phase measuring instrument.

(v) Q Measurement from inflection points of the resonance curve

The tuned circuit behaves most nearly like a linear network in the neighbourhood of the two frequencies on the resonance curve and therefore, the second derivative, is zero at the inflection points of the curve. To a very good approximation, it can be shown that $Q_L = f_0/(\sqrt{3} \Delta f)$ for the response curve, where Δf is frequency

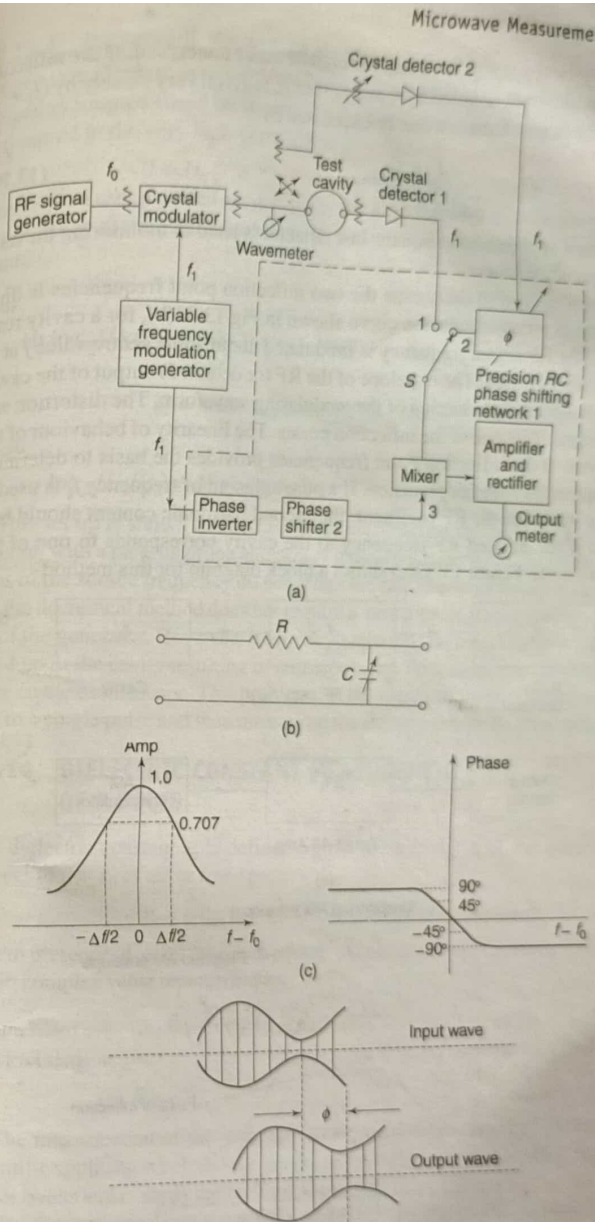


Fig. 13.31 (a) Phase-shift method of measurement of Q (b) Precision RC phase shifting network (c) Transmission characteristics of single tuned resonator (d) Phase change of transmitted signal

difference between the inflection points of the curve concerned. If the inflection point frequencies are denoted by f_1 and f_2 , then f_0 is given very closely by $(f_1 + f_2)/2$, so that the above equation can be expressed by

$$Q_L = \frac{f_1 + f_2}{2\sqrt{3|f_1 - f_2|}} \quad (13.79)$$

The equation applies when a square-law detector is used in monitoring the resonator frequency response.

A general method to determine the two inflection point frequencies is illustrated in the power transmission curve shown in Fig. 13.32(b), for a cavity resonant at f_0 . The RF signal frequency is modulated about some centre value f at an audio frequency f_1 rate. The envelope of the RF (or detected) output of the cavity will be a distorted reproduction of the modulating waveform. The distortion will be a minimum if f is one of the inflection points. The linearity of behaviour of the tuned circuit at the inflection point frequencies provides the basis to determine these frequencies with fair precision. If a pure sinusoid of frequency f_1 is used to frequency modulate the RF oscillator, the second harmonic content should be a minimum if the applied RF frequency to the cavity corresponds to one of the inflection points. Figure 13.32(a) shows a block diagram for this method.

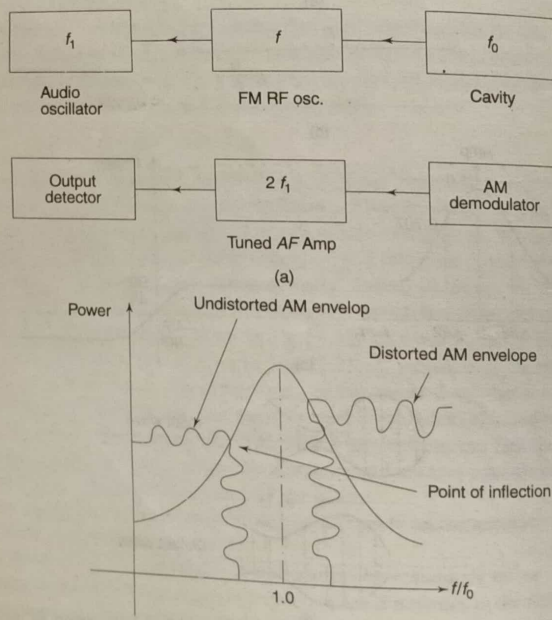
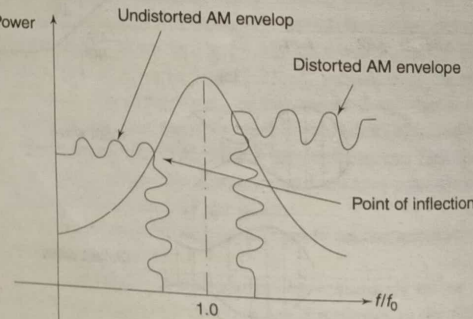


Fig. 13.32 (a) Inflection point method of measurement of Q (b) Inflection point of resonance curve of cavity

(b)



13.13.4 Decrement Method of Measurement of Q

Since it is difficult to measure VSWR or transmission in a very high Q system, a method is adopted based on measuring the time rate of decay of microwave energy stored in the very high Q resonator :

$$U = U_0 e^{-(\omega_0 t/Q)}$$

This method uses a pulsed excitation for the cavity system and observation of the rate of decay of the oscillations from U_1 to U_2 between exciting pulses at times t_1 and t_2 .

Thus

$$10 \log_{10}(U_1/U_2) = 4.343 \omega_0(t_2 - t_1)/Q \quad (13.80)$$

or,

$$Q = 8.686\pi f_0 \Delta t/A = 27.3 f_0 \Delta t/A \quad (13.82)$$

where

$$10 \log_{10}(U_1/U_2) = A, t_2 - t_1 = \Delta t \quad (13.83)$$

This set up is shown in Fig. 13.33. An oscilloscope technique is used in conjunction with a pick-up probe and power indicating equipment. Since the fluctuations of the source frequency do not affect the rate of energy decay in the resonator, the decrement method does not require a very high degree of frequency stability of the generator. However, frequency variations do affect the level of energy build up in the cavity resulting in corresponding fluctuations in the decay curve trace on the oscilloscope. This problem can be overcome by photographing a trace due to a single pulse and then measuring the decay time on the photograph.

13.14 DIELECTRIC CONSTANT MEASUREMENT OF A SOLID

The dielectric constant ϵ_r is defined by the permittivity ϵ of the material with respect to that ϵ_0 of air or free space

$$\epsilon_r = \epsilon/\epsilon_0, \epsilon_0 = (10^{-9}/36\pi) \text{ farad/m} \quad (13.84)$$

Due to presence of non-zero conductivity, dielectric material exhibits loss, resulting in complex value represented by

$$\epsilon_r = \epsilon'_r + j \epsilon''_r \quad (13.85)$$

The loss tangent

$$\tan \delta = \epsilon''_r / \epsilon'_r \quad (13.86)$$

The measurement of the complex dielectric constant is required not only in scientific application but also for industrial applications such as microwave heating or ovens and to study the biological effects of microwaves.

The dielectric constant is not independent of frequency. Generally, the variation of ϵ_r with frequency is sufficiently gradual so that it can be considered to be

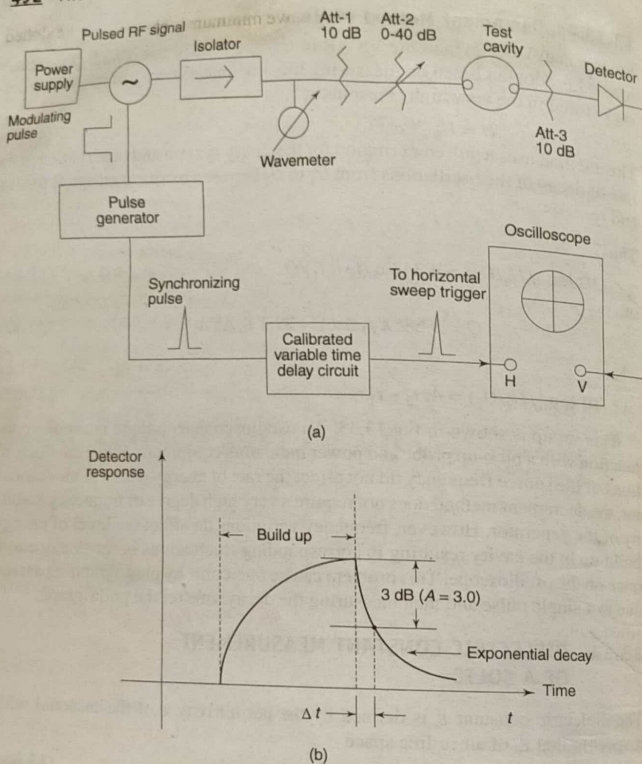


Fig. 13.33 (a) Decrement method of measuring Q (b) Transient response of a cavity

constant over a fairly wide frequency band for most common microwave applications. On the other hand, the per cent variation in ϵ_r'' is almost always greater than that of ϵ_r' , so that ϵ_r'' should be measured near the frequency or frequencies of interest.

There are several methods available for dielectric constant measurement. The following sections describe two commonly used methods: the waveguide method and cavity perturbation method.

13.14.1 Waveguide Method *lossless material*

In this method it is assumed that the material is lossless. A dielectric sample AB completely fills a length of the waveguide and the end is terminated in a short as

Microwave Measurements 493
shown in Fig. 13.34. A voltage standing wave minimum is observed in the slotted line at C (say).

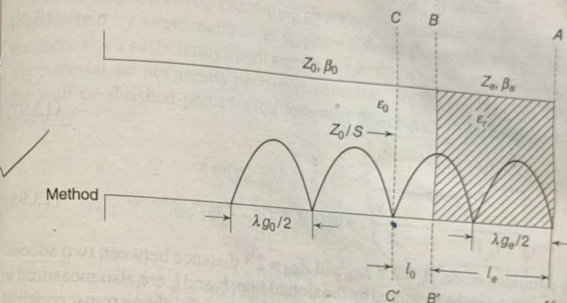


Fig. 13.34 Waveguide method

Let

$$l_e = AB = \text{the dielectric sample length} \quad (13.87)$$

$$l_0 = BC \quad (13.88)$$

Then the distance of V_{\min} from short circuit is $l_0 + l_e = AC$. For a dielectric filled guide of characteristic impedance Z_e , input impedance at B is purely reactive,

$$Z_{in}' = jZ_e \tan \beta_e l_e$$

where β_e is the propagation constant.

Using this Z_{in}' as termination at B, input impedance at C for the empty guide

$$Z_{inC} = \frac{Z_{in}' + jZ_0 \tan \beta_0 l_0}{Z_0 + jZ_{in}' \tan \beta_0 l_0} = 0, \text{ at } V_{\min} \text{ point} \quad (13.90)$$

Therefore,

$$Z_{in}' + jZ_0 \tan \beta_0 l_0 = 0 \quad (13.91)$$

or,

$$jZ_e \tan \beta_e l_e + jZ_0 \tan \beta_0 l_0 = 0 \quad (13.92)$$

or,

$$Z_0 \tan \beta_0 l_0 = -Z_e \tan \beta_e l_e \quad (13.93)$$

Assuming nonmagnetic dielectric in the waveguide,

$$\frac{Z_0}{Z_e} = \frac{\beta_e}{\beta_0} \quad (13.94)$$

or

$$Z_0 = \frac{\beta_e Z_e}{\beta_0} \quad (13.95)$$

Substituting this value in Eq. 13.93

$$\frac{\beta_e Z_e}{\beta_0} \tan \beta_0 l_0 = -Z_e \tan \beta_e l_e \quad (13.96)$$

or,

$$\frac{l_0 \tan \beta_0 l_0}{\beta_0 l_0} = -\frac{l_e \tan \beta_e l_e}{\beta_e l_e} \quad (13.97)$$

or,

$$\frac{l_0 \tan Y}{l_e Y} = -\frac{\tan X}{X}; \text{ where } X = \beta_e l_e, Y = \beta_0 l_0; \quad (13.98)$$

For dominant mode, $\beta_0 = 2\pi/\lambda g_0$ and $\lambda g_0 = 2 * \text{distance between two successive } V_{\min}$ which can be measured by the slotted line. l_0 and l_e are also measured in the slotted line. Therefore, the left hand side (α say) of the above transcendental Eq. 13.98 is known and it can be written as

$$(\tan X)/X = -\alpha \quad (13.99)$$

The above equation can be solved for determining $X = \beta_e l_e$. Now

$$\beta_e = \frac{2\pi}{\lambda_{ge}} = \frac{2\pi}{\lambda_0} \sqrt{\epsilon_r - \left(\frac{\lambda_0}{\lambda_e}\right)^2}, \lambda_e = 2a \quad (13.100)$$

where a is the waveguide broadwall dimension.

Since β_e is known, ϵ_r can be determined from above equation. This equation has infinite number of solutions for ϵ_r . Hence two different lengths of sample are taken for two sets of solutions.

For length $l_e : X = X_1, X_2, \dots$

$\epsilon_r = \epsilon_{r1}, \epsilon_{r2}, \dots$

For length $l'_e : X = X'_1, X'_2, \dots$

$\epsilon'_r = \epsilon'_{r1}, \epsilon'_{r2}, \dots$

The desired value of ϵ_r is the solution which is common for the two samples.

13.14.2 Cavity Perturbation Method

Cavity perturbation techniques are highly sensitive and accurate and therefore, particularly advantageous in the determination of the dielectric constant and small loss tangents.

In the cavity perturbation technique, a small volume of the test sample is introduced in a cavity resonator at the position of maximum E-field for the measurement of ϵ (and at maximum H-field for the measurement of μ). Since the volume of the sample is small, the field in the cavity is assumed to remain undisturbed.

But introduction of dielectric sample changes the resonance frequency and loss. These changes are reflected in the change of Q of the cavity from its unperturbed value. All these changes are related to the dielectric constant and the tangent.

Let the original cavity containing air having ϵ_0, μ_0 and resonance frequency f_0 is perturbed by some material ϵ, μ placed inside the cavity at E_{max} and $H=0$ position. For a sufficiently small sample the fields in the cavity outside the dielectric material are not greatly perturbed from those for the empty cavity case. Then the well established perturbation formulae for change in frequency and Q are given by

$$\omega - \omega_0 = \frac{\omega(\epsilon' - 1) \int |E_0|^2 dv}{V_s} \quad (13.101)$$

$$\left(\frac{1}{Q}\right) = \frac{\epsilon'' |E_0|_{V_s}^2 V_s}{\int |E_0|^2 dv} \quad (13.102)$$

where

E_0, ω_0 = the field and resonant frequency of the original cavity

E, ω = the corresponding quantities of the perturbed cavity

V_c, V_s = volumes of the empty cavity and the sample filling the cavity, respectively

Assuming small perturbation, ω can be replaced by ω_0 and the simplified relations are

$$\frac{\Delta\omega_0}{\omega_0} = \frac{(\epsilon' - 1) |E_0|_{V_s}^2 V_s}{2 \int |E_0|^2 dv} \quad (13.103)$$

$$\left(\frac{1}{Q}\right) = \frac{\epsilon'' |E_0|_{V_s}^2 V_s}{\int |E_0|^2 dv} \quad (13.104)$$

where $|E_0|_{V_s}$ has been assumed constant over the region of integration throughout the small sample and

$$\left(\frac{1}{Q}\right) = \left(\frac{1}{Q_c}\right) - \left(\frac{1}{Q_s}\right) \quad (13.105)$$

Here

$Q_c = Q$ of the unperturbed cavity

$Q_s = Q$ of the perturbed cavity

In principle, any type of cavity either rectangular or circular can be used with excitation by suitable mode. The following criteria are important.

- The cavity Q should be as high as possible to enhance the accuracy of the measurement and this is very stringent, particularly in low loss materials.
- The mode of operation should be such that the dielectric sample is conveniently placed at a uniform field region E_{\max} where $H = 0$ for the measurement of ϵ' and ϵ'' . Otherwise, if $H \neq 0$ in the perturbed region, complex permeability of the magnetically lossy material will add to frequency shift and RF loss in addition to the contribution offered by complex ϵ . It will be extremely troublesome to mathematically relate the individual contributions (reverse is the case for the measurement of μ).
- The accuracy of the method depends on the smoothness of the sample, and fitness of the sample in the cavity. The smaller the sample, the more critically the accuracy will depend upon the sample irregularities. It is, therefore, necessary to machine the sample very carefully for smoothness and size.

In view of the above, rectangular cavity in TE_{103} mode and circular cavity in TM_{010} mode is found suitable in this technique. Both the cavities thus produce E_{\max} and $H = 0$ at the centre where the dielectric samples in the form of a thin rod are placed inside the cavity transversely as post parallel to E-field as shown in Fig. 13.35. With this combination, the perturbation relations are described as follows.

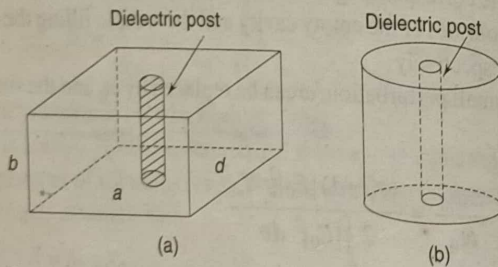


Fig. 13.35 Cavity perturbation method (a) Rectangular cavity TE_{103} (b) Circular cavity TM_{010}

TE_{103} rectangular cavity The non-zero field components for TE_{103} mode in the rectangular cavity $a \times b \times d$ are E_y , H_x and H_z only. Since the sample length is parallel to y , only E_y is required for finding ϵ_r ,

$$E_y = \frac{\lambda}{2a} \sin(\pi x/a) \sin(3\pi z/d) \quad (13.106)$$

If the sample is placed at $x = a/2$, $z = d/2$

$$\begin{aligned} |E_0|^2 &= |E_y|^2 = \left(\frac{\lambda}{2a}\right)^2 \\ V_s x &= a/2 \\ z &= d/2 \end{aligned} \quad (13.107)$$

and

$$\begin{aligned} \int_{V_c} |E_0|^2 dv &= \left(\frac{\lambda}{2a}\right)^2 \int_0^a \int_0^b \int_0^d \sin^2\left(\frac{\pi x}{a}\right) \sin^2\left(\frac{3\pi z}{d}\right) dx dy dz \\ &= \left(\frac{\lambda}{2a}\right)^2 \frac{abd}{4} \end{aligned} \quad (13.108)$$

Substituting Eq. 13.108 and Eq. 13.109 in Eqs. 13.104 and 13.105,

$$\frac{\Delta f_0}{f_0} = -2(\epsilon_r' - 1) \frac{V_s}{V_c} \quad (13.109)$$

$$\left(\frac{1}{Q}\right) = 4\epsilon_r'' \frac{V_s}{V_c} \quad (13.110)$$

or,

$$\epsilon_r' = 1 + 0.5 \left(\frac{V_c}{V_s}\right) \frac{f_0 - f}{f_0} \quad (13.111)$$

$$\epsilon_r'' = 0.25 \left(\frac{V_c}{V_s}\right) \left(\frac{1}{Q_c} - \frac{1}{Q_s}\right) \quad (13.112)$$

TM_{010} circular cavity For the circular cavity in TM_{010} mode $E_p = 0 = E_\phi$ and E_z is parallel to the length of the sample rod which is introduced axially. It can be shown in a similar way

$$\epsilon_r' = 0.539 \left(\frac{V_c}{V_s}\right) \left(\frac{\Delta f_0}{f_0}\right) + 1$$

$$\epsilon_r'' = 0.269 \left(\frac{V_c}{V_s}\right) \Delta \left(\frac{1}{Q}\right)$$

The unique feature of the TM_{010} mode is that its resonant frequency is independent of the length and therefore design is very simple.

13.15 MEASUREMENTS OF SCATTERING PARAMETERS OF A NETWORK

S-parameters can be conveniently measured following the Deschamps method which utilises measured values of complex input reflection coefficients under a number of reactive terminations. In this section measurements of S-parameters of a general two-port network and a four-port network called the magic-T are described.

13.15.1 S-Parameters of a Two-Port Network

The output end of the two-port network is terminated with a short circuit plunger to vary the reactive termination by moving the plunger in steps of at least 1/8th of

the guide wavelength and the corresponding input reflection coefficients are measured. When the attenuation coefficient α in the line is small and the change of total length of the line is less than one guided wavelength, the points P 's of the corresponding measured reflection coefficients describe an average circle on the polar chart with centre O' and radius CP as shown in Fig. 13.36. However, for a lossless line $\alpha = 0$ and the reflection coefficients will describe a perfect circle. The reflection coefficients can be measured using a network analyser and reflection bridge set-up. The each pair of reflection coefficient points P 's, diametrically opposite, are joined and the lines of intersection O' is marked. CO' is joined. Two perpendicular lines at C and O' are drawn to intersect the circle at Q and P respectively. PQ is joined to intersect CO' at S_{11} . A line $S_{11}E$ parallel to $O'P$ is drawn to meet the circle at E . It can be shown that

$$|S_{11}| = |OS_{11}| \quad (13.115)$$

and

$$|S_{12}| = \frac{|S_{11}E|}{\sqrt{\rho \cdot R}} \quad (13.116)$$

where R is the radius of the circle and $\rho = \exp(-2\alpha l)$, the input reflection coefficient with output end of the line short circuited. The attenuation coefficient can be determined from the following equation when experiments are performed using two widely different lengths l and l' of the line

$$\alpha = \frac{1}{2(l - l')} \ln \left(\frac{R|S_{11}E|^2}{R'|S_{11}E'|^2} \right) \quad (13.117)$$

For $|S_{22}|$ and $|S_{21}|$, measurements are carried out by interchanging the ports.

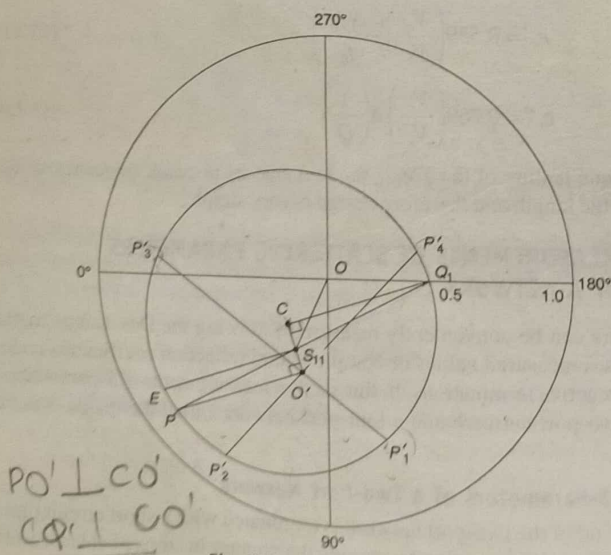


Fig. 13.36 Deschamps method

13.15.2 S-Parameters of a Magic-T

The S-parameters of a matched magic-T can be determined using the Deschamp's method by measuring the reflection coefficients at different ports under specific termination of other ports as explained below (Fig. 13.37).

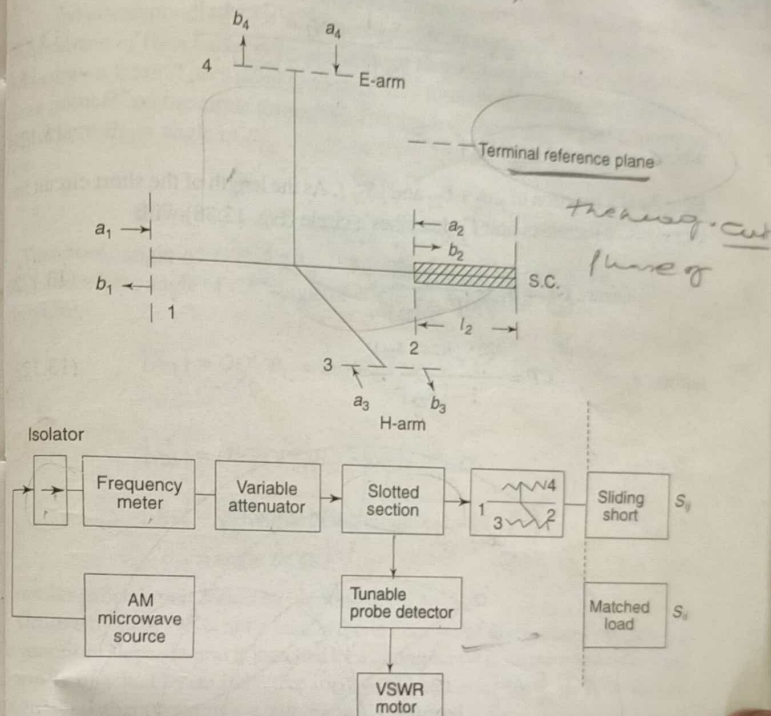


Fig. 13.37 Experimental set-up for S-parameters measurement of Magic-T

(a) *Measurement of S_{ii}* : The diagonal elements are determined from the slotted line measurement of the VSWR S_i at the corresponding port with all other ports matched terminated.

$$|S_{ii}| = (S_i - 1) / (S_i + 1) \quad (13.118)$$

(b) *Measurement of S_{ij} ($i \neq j$)*: To measure S_{12} , ports 3 and 4 are match terminated and port 2 is terminated in a short circuit plunger when the input is fed at port 1. At the reference plane of port 2, the reflection coefficient will always be equal to 1 in magnitude but its phase will vary continuously with the distance of the short position from the same reference plane, leading to a reflection coefficient $F_2 = -e^{j2\theta_2}$. Since $S_{12} = S_{21}$ for an isotropic medium,

$$\Gamma_1 = S_{11} - \frac{S_{12}^2 e^{j2\theta_2}}{1 + S_{22} e^{j2\theta_2}} \quad (13.119)$$

or,

$$\Gamma_1 = S_{11} + \frac{S_{12}^2 S_{22}^*}{1 - |S_{22}|^2} + \frac{S_{12}^2 e^{j(2\phi - \theta_{22})}}{1 - |S_{22}|^2} \quad (13.120)$$

where $S_{22}^* = |S_{22}| e^{-j\theta_{22}}$

Here 2ϕ is a function of $2\theta_2 + \theta_{22}$ and $|S_{22}|$. As the length of the short circuit line increases, ϕ increases and Γ_1 describes a circle (Fig. 13.38) with

$$\text{Centre } OC = S_{11} + \frac{S_{12}^2 S_{22}^*}{1 - |S_{22}|^2} \quad (13.122)$$

radius $CP = \frac{S_{12}^2 e^{j(2\phi - \theta_{22})}}{1 - |S_{22}|^2} \quad (13.123)$

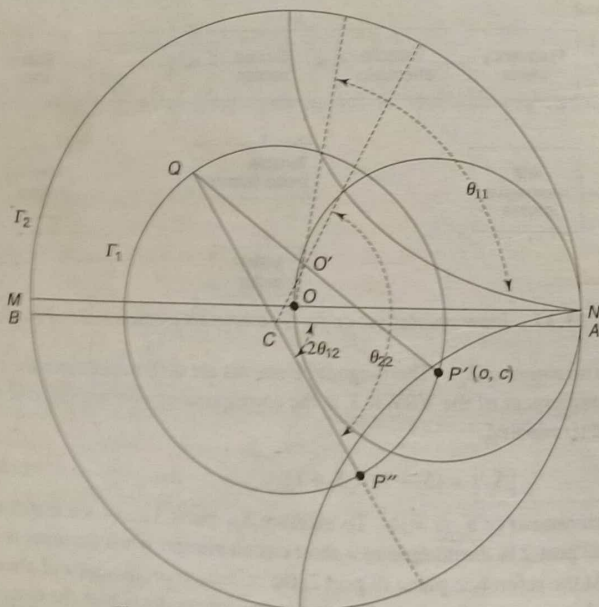


Fig. 13.38 Deschamps's circle for magic-T

The experimental measurement procedure is as follows:

1. Ports 2, 3 and 4 are matched terminated and S_{11} is measured directly at

port 1. $S_{11} = OO'$ is located on the Smith chart where O is the 'iconocentre'.

2. Placing a sliding short at port 2, $\theta_2 = \beta l_2$ is varied to obtain Γ_1 circle on the Smith chart. The centre C is determined on the diagram.
3. Placing open circuit at the reference plane of port 2 ($\theta_2 = \pi/2$, $l_2 = \lambda_g/4$)

the corresponding $\Gamma_1 = \Gamma'_1$ is noted and indicated on Γ_1 circle as P' . Construction of Deschamp's circle is done in the following manner. A straight line is drawn from P' to a point Q on the circle through O' and another line from Q to a point P'' on the circle through C . The angle of the phase or CP'' is equal to $2\theta_{12}$, where θ_{12} = angle of S_{12} . Now

$$O'C = OC - OO' = S_{12}^2 S_{22}^* / (1 - |S_{22}|^2) \quad (13.124)$$

Therefore, angle of $O'C = 2\theta_{12} - \theta_{22}$. Since angle of $CP'' = 2\theta_{12} = \text{Angle } BCQ$, therefore, angle of CP'' -angle of $O'C = \theta_{22} = \text{Angle } P''CO'$. Therefore,

$$|S_{11}| = OO', \theta_{11} = \text{angle of } NOO' \quad (13.125)$$

and

$$|S_{22}^*| = O'C/CP'', \theta_{22} = \text{angle } P''CO' \quad (13.126)$$

$$|S_{12}| = \sqrt{\text{Radius of the circle} \times (1 - |S_{22}|^2)} \quad (13.127)$$

$$\theta_{12} = \text{angle } BCQ/2 \quad (13.128)$$

A similar procedure is followed for other ports.

Ordinarily magic-T is not a matched one because of discontinuity presents at the junction. Hence H-arm is matched by a tuning screw from the bottom wall and E-arm is matched by an inductive iris by trial and error method. With this arrangement other two arms are automatically matched.

13.16 MICROWAVE ANTENNA MEASUREMENTS

The most important parameters required to be measured to determine the performance characteristics of microwave antennas are radiation amplitude patterns, radiation phase patterns, absolute gain, directivity, radiation efficiency, beamwidth, input impedance, bandwidth and polarisations. The accurate measurement methods for these parameters require standard antenna test ranges.

13.16.1 Antenna Test Ranges

There are two basic antenna test ranges used for antenna measurements. These are indoor and outdoor test ranges. Usual indoor test range is an anechoic chamber which consists of a rectangular volume enclosed by microwave absorber walls. These walls reduce reflections from the boundary walls and increases the measurement accuracy. Microwave absorbers are carbon impregnated

polyurathene foam in the shape of pyramids. The materials are expensive for lower frequency ranges because the typical size of pyramid is nearly 5'-6' for 100 MHz. Most of the antenna parameters to be measured require uniform plane wave field incidence on the test antenna placed at a far field distance from a transmitting antenna. Consequently the requirement of a large space limits the use of the costly indoor facility. Special indoor ranges such as compact range and smaller distance by means of an offset fed reflector antenna having a special edge geometry. The latter one uses mathematical computations of the near field measurement data to obtain the far field information. Both these methods are very costly and have several limitations. In this section, far field outdoor test range is discussed for antenna parameter measurements.

Outdoor antenna test range The most popular microwave antenna test range is the free space outdoor range in which the antennas are mounted on tall towers as shown in Fig. 13.39. The reflections from the surrounding environment are reduced by

1. Selecting the directivity and side lobe level of the transmitting antenna.
2. Making line-of-sight between the antennas obstacle free.
3. Absorbing or redirecting the energy that is reflected from the range surface or from any obstacle.

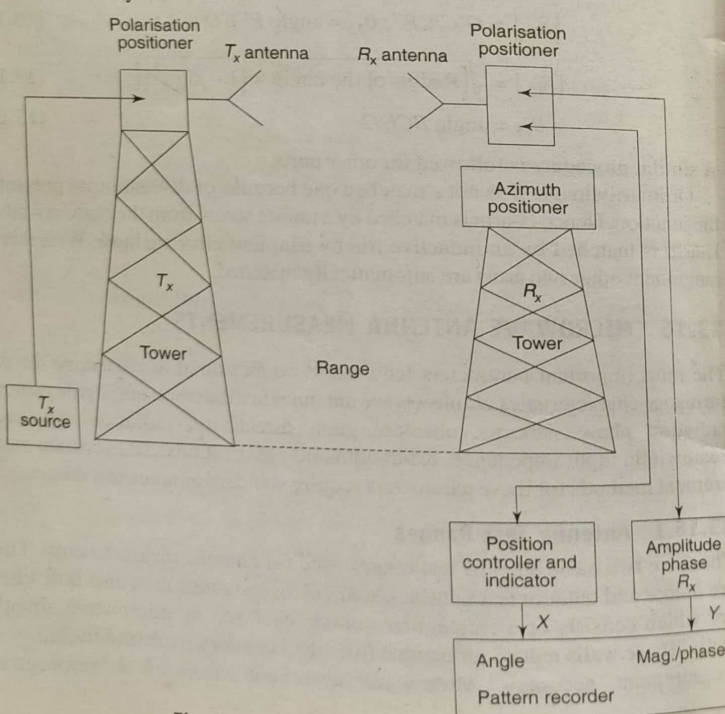


Fig. 13.39 Outdoor antenna test range

13.16.2 Radiation Pattern Measurements

The radiation pattern is a representation of the radiation characteristics of the antenna as a function of elevation angle θ and azimuthal angle ϕ for a constant radial distance and frequency. The three-dimensional pattern is decomposed into two orthogonal two-dimensional patterns in E and H field planes where the Z-axis is the line joining the transmitting and receiving antennas and perpendicular to the radiating apertures. Due to the reciprocal characteristics of antennas, the measurements are performed with the test antenna placed in the receiving mode. The source antenna is fed by a stable source and the received signal is measured using a receiver. The output of the receiver is fed to Y-axis input of an XY recorder. The receiving antenna positioner controller plane and the angle information is fed to X-axis input of the XY recorder. Thus the amplitude vs angle plot is obtained from the recorder output.

Initially two antennas are aligned in the line of their maximum radiation direction by adjusting the angle and height by the controller and antenna mast. Effects of all surroundings are removed or suppressed through increased directivity and low side lobes of the source antenna, clearance of LOS, and absorption of energy reaching the range surface.

The following precautions are taken for better accuracy in the measurements:

1. Effects of coupling between antennas—inductive or capacitive—causes error in measurement. The former exists at lower microwave frequencies and negligible if range $R \geq 10 \lambda$. Mutual coupling due to scattering and reradiation of energy by test and source antenna causes error in measurement.
2. Effect of curvature of the incident phase front produces phase variation over the aperture of test antenna and this restricts the range R . For a phase deviation at the edge $\leq \pi/8$ radians, $R \leq 2D^2/\lambda$, where D is the maximum size of the aperture.
3. Effect of amplitude taper over the test aperture will give deviation of the measured pattern from the actual. This occurs if the illuminating field is not constant over the region of the test aperture. Tolerable limit of amplitude taper is 0.25 dB, for which decrease in gain is 0.1 dB.
4. Interference from spurious radiating sources should be avoided.

13.16.3 Phase Measurement

The phase of the radiated field is a relative quantity and is measured with respect to a reference as shown in Fig. 13.40. This reference is provided either by coupling a fraction of the transmitted signal to the reference channel of the receiver or by receiving the transmitted signal with a fixed antenna placed near the test antenna. The fixed antenna output is fed to the reference channel of the receiver and the phase pattern is recorded as the antenna under test is rotated in the horizontal plane.

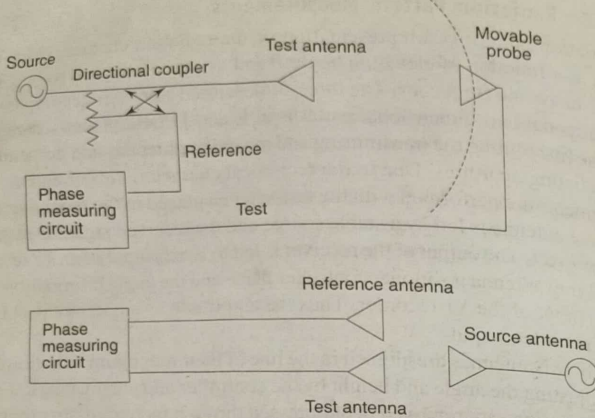


Fig. 13.40 Phase pattern measurement set-up

13.16.4 Phase Centre Measurement

When an antenna radiates, there is an equivalent point in the antenna geometry which represents the radiation centre. At the far field region the phase pattern of this antenna remains constant with angle when measured with respect to this point. Therefore, the phase centre of the test antenna is determined by positioning the rotational axis of the test antenna mast such that the phase pattern within the main beam remains constant.

13.16.5 Beamwidth

The beamwidth of the antenna is calculated from the angle subtended by the 3 dB or 10 dB points on the both sides of radiation maximum in the main beam.

13.16.6 Gain Measurements

The gain is the most important parameter to be measured for microwave antennas because it is used directly in the link calculations. There are three basic methods that can be used to measure the gain: standard antenna method, two antenna method and three antenna method.

Standard antenna method This method uses two sets of measurements with the test and standard gain antennas. Using the test antenna of gain G_r in receiving mode, the received power P_r is recorded in a matched recorder. The test antenna is then replaced by a standard gain antenna of gain G_s and the received power P_s is again recorded without changing the transmitted power and geometrical configuration. Then

$$\frac{P_r}{P_s} = \frac{G_r}{G_s}$$

$$G_r(\text{dB}) = G_s(\text{dB}) + 10 \log\left(\frac{P_r}{P_s}\right) \quad (13.129)$$

Thus by measuring the received power with test and standard gain antennas and knowing gain G_s of the standard gain antenna, the gain of the test antenna can be found.

Two antenna method In this method the signal is transmitted from a transmitting antenna of gain G_t and the signal is received by the test antenna of gain G_r placed at far-field distance R . The received power is expressed by

$$P_r = \frac{P_t G_t G_r \lambda^2}{(4\pi R)^2}$$

or,

$$G_r(\text{dB}) + G_t(\text{dB}) = 20 \log\left(\frac{4\pi R}{\lambda}\right) + 10 \log\left(\frac{P_r}{P_t}\right); \quad (13.130)$$

where P_r is the received power and P_t is the transmitted power. When the two antennas are selected identical, $G_t = G_r$, so that

$$G_r(\text{dB}) = G_t(\text{dB}) = 10 \log\left(\frac{4\pi R}{\lambda}\right) + 5 \log\left(\frac{P_r}{P_t}\right); \quad (13.131)$$

By measuring R , λ and P_r/P_t , the gain G_r can be determined.

Three antenna method In the two antenna method if the measuring systems are not exactly identical, error will be introduced. Hence the three antenna method is the most general method to find gain of all the three antennas. Any two antennas are used at a time i.e. 1 and 2, 2 and 3, and 3 and 1, respectively. The following equations can be developed for the received and transmitted powers

$$G_1(\text{dB}) + G_2(\text{dB}) = 20 \log\left(\frac{4\pi R}{\lambda}\right) + 10 \log\left(\frac{P_{r2}}{P_{t1}}\right) \quad (13.132)$$

$$G_2(\text{dB}) + G_3(\text{dB}) = 20 \log\left(\frac{4\pi R}{\lambda}\right) + 10 \log\left(\frac{P_{r3}}{P_{t2}}\right) \quad (13.133)$$

$$G_3(\text{dB}) + G_1(\text{dB}) = 20 \log\left(\frac{4\pi R}{\lambda}\right) + 10 \log\left(\frac{P_{r1}}{P_{t3}}\right) \quad (13.134)$$

Since R and λ are known and (P_r/P_t) 's are measured, the right hand side of the above equations are known. Then three unknown quantities G_1 , G_2 and G_3 can be determined from the three equations.

A typical block diagram of the measurement set-up for two and three antenna methods are shown in Fig. 13.41.

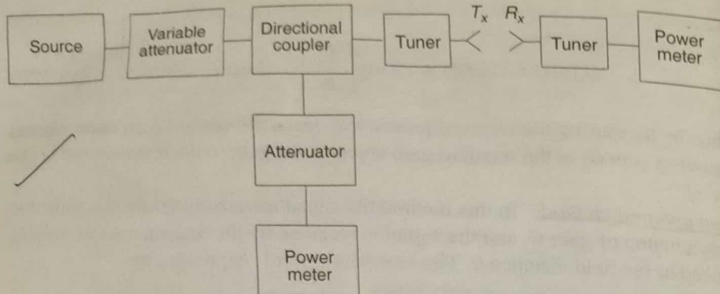


Fig. 13.41 Block diagram of antenna gain measurements

For accuracy of the measurements, care must be taken so that

1. All antennas meet the far field criteria : $R \geq 2D^2/\lambda$.
2. The antennas are aligned for bore-sight radiation face-to-face.
3. The measuring system is frequency stable.
4. Impedance mismatched in the system components is minimum.
5. Polarisation mismatch is minimum.
6. Reflection from various background and support structure is minimum.

13.16.7 Directivity Measurements

The directivity of an antenna can be determined from the measurements of its radiation pattern in two principal planes, E and H planes and finding the half-power beamwidths θ_E and θ_H degree in these planes, respectively.

$$D_0 = \frac{41,253}{\theta_E \theta_H} \quad \text{or,} \quad \frac{72,815}{\theta_E^2 + \theta_H^2} \quad (13.135)$$

This method is accurate for the antennas having negligible side lobes.

13.16.8 Radiation Efficiency

The radiation efficiency = $\frac{\text{Total power radiated, } P_{\text{rad}}}{\text{Total power accepted at its input}}$

$$= \frac{P_{\text{rad}}}{P_{\text{in}} - P_{\text{ref}}} = \frac{\text{Gain}}{\text{Directivity}} \quad (13.136)$$

where P_{in} is the input power and P_{ref} is the reflected power at the input. Therefore, the radiation efficiency can be determined from the measurement of gain and directivity.

13.16.9 Polarisation Measurements

The polarisation of an antenna is conveniently measured by using it in the transmitting mode and probing the polarisation by a dipole antenna in the plane that contains the direction of the electric field as shown in Fig.13.42. The dipole is

rotated in the plane of polarisation and the received voltage pattern is recorded and analysed as follows.

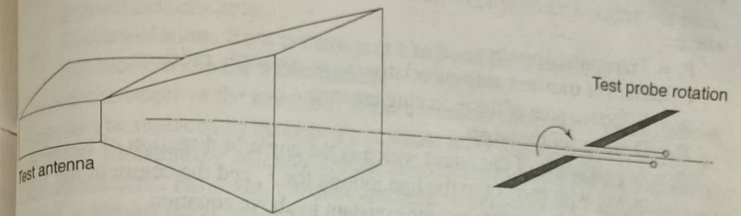


Fig. 13.42 Polarisation measurements

Linear polarisation For linear polarisation, the output voltage pattern will be a figure of eight.

Circular polarisation For circular polarisation, the output voltage pattern will be a circle.

Elliptical polarisation For an elliptical polarisation, the nulls of the figure of eight are filled and a dumb-bell polarisation curve is obtained which will be tilted and a polarisation ellipse can be drawn as shown by dashed curve in Fig.13.43. The sense of rotation of the circular and elliptical polarisations can be determined by comparing the responses of two circularly polarised antennae, one left and the other rightwise rotation. The polarisation of the test antenna will be the same as that of one of these two directions for which the response is larger.

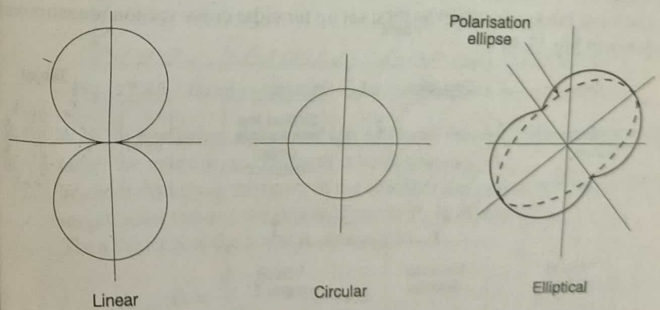


Fig. 13.43 Polarisation patterns

13.17 RADAR CROSS-SECTION (RCS) MEASUREMENTS

The radar cross-section of a target is defined by

$$\sigma = \frac{4\pi \times \text{Power re-radiated per unit solid angle}}{\text{Incident power density}} \quad (13.137)$$

and is expressed in terms of received power

$$P_r(\theta) = \frac{P_t G_t A_e \sigma(\theta)}{(4\pi R^2)^2} \quad (13.138)$$

where

 P_t = Transmitted power G_t = Gain of transmit antenna relative to an isotropic radiator A_e = Effective area of the receiving antenna R = Distance of the target θ = Aspect angle of the target which is the angle of direction of re-radiated power with respect to the line joining the T_x and the centre of the target

When all the factors remain constant in above equation

$$\sigma(\theta) = K P_r(\theta) \quad (13.139)$$

where K is a constant. Normalising with respect to the angle $\theta = 0$,

$$\frac{\sigma(\theta)}{\sigma(0)} = \frac{P_r(\theta)}{P_r(0)} \quad (13.140)$$

Thus by measuring the received power, the radar cross-section of a target placed at far field location, can be determined.

There are two basic radar cross-section terms i.e. monostatic or back scattering cross-section and bistatic cross-section. The former is defined for the reflected signal received by the common transmit/receive antenna. The other one is defined when the scattered signal is measured in the forward direction other than towards the source end. We will be interested in the back scattered radar cross-section in this chapter.

The basic laboratory experimental set up for radar cross-section measurement is shown in Fig. 13.44.

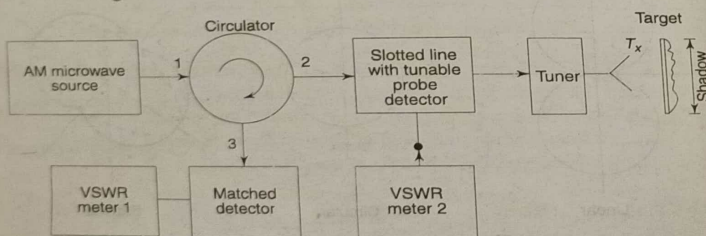


Fig. 13.44 Basic radar cross-section measurement set-up

Since signals reflected from the background cause error in the measurement, the tuner is adjusted to obtain minimum reading in VSWR meter-1 ($S < 1.05$) without the target present. Without disturbing the tuner, the target is now positioned and received signal strength is adjusted to read $S = 1$ in the VSWR meter-2 when $\theta = 0^\circ$. The target is now rotated in azimuthal angular directions and corresponding readings in the VSWR meter-2 are noted to obtain normalised RCS vs angle information.

The possible sources of error in the above method are

- Experiments 509
- When background cancellation was done by using the tuner, the target shadow region at its back contributed to background echo which is not present when the target was positioned. This produces imperfect background cancellation.
 - Finite isolations from isolator port 1 to 3 and from port 2 to 1 produce error in the measurement.

In order to improve the isolation between transmit and receive signal, the circulator can be replaced by arranging a separate receiving antenna system by the side of the transmitting antenna. Under these circumstances the RCS is called quasi-monostatic. However, transmit and receive antennas are considered to be located at almost same origin when the target is at far away from the antennas.

For better cancellation of actual background echo, RCS of a target is often defined in terms of an equivalent sphere whose $\text{RCS} = \sigma_{\text{sphere}}$ is precisely known and is independent of aspect angle. Following measurements are recommended inside an anechoic chamber of low reflection coefficient as shown in Fig. 13.45.

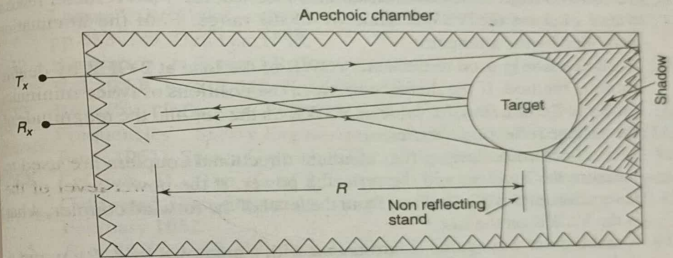


Fig. 13.45 Quasi-monostatic radar cross-section measurements

- With an equivalent sphere of almost same vertical cross-section of the target the return signal strength is measured as P_{rs} .
- Without disturbing anything in the chamber the sphere is replaced by the target under test and the received power P_{rt} is measured.

Then the RCS of the target is obtained as

$$\sigma_{\text{target}}(\theta) = \frac{P_{rt}(\theta)}{P_{rs}} \times \sigma_{\text{sphere}} \quad (13.141)$$

EXERCISES

- The signal power at the input of a device is 10 mW. The signal power at the output of the same device is 0.20 mW. Calculate the insertion loss in dB of this component.
- A crystal detector generates a signal of 10 mV for an incident microwave power of -25 dBm. What is the detector sensitivity in mV/mW? Why is